Synthesis and Applications of Amino-Functionalized Carbon Nanomaterials

Marina Garrido, Lorenzo Gualandi, Simone Di Noja, Giacomo Filippini, Susanna Bosi and Maurizio Prato

Carbon-based nanomaterials (CNMs) have attracted considerable attention in the scientific community both from a scientific and an industrial point of view. Fullerenes, carbon nanotubes (CNTs), graphene and carbon dots (CDs) are the most popular forms and continue to be widely studied. However, the general poor solubility of many of these materials in most common solvents and their strong tendency to aggregate remains a major obstacle in practical applications. To solve these problems, organic chemistry offers a formidable help, through the exploitation of tailored approaches, especially when aiming at the integration of nanostructures in biological systems. According to our experience with carbon-based nanostructures, the introduction of amino groups is one of the best trade-offs for the preparation of functionalized nanomaterials. Indeed, amino groups are well-known for enhancing the dispersion, solubilization, and the processability of materials, in particular of CNMs. Amino groups are characterized by basicity, nucleophilicity, and formation of hydrogen or halogen bonding. All these features unlock new strategies for the interaction between nanomaterials and other molecules. This integration can occur either through covalent bonds (e.g., *via* amide coupling) or in a supramolecular fashion. In the present Feature Article, the attention will be focused through selected examples of our approach to the synthetic pathways necessary for the introduction of amino groups in CNMs and the subsequent preparation of highly engineered *ad hoc* nanostructures for practical applications.

1. Functionally engineered nanomaterials: a background

Nanoscience is an intersectorial discipline rooted in the fields of physics, chemistry, biology, medicine and engineering. The principal aim of this branch of science is to develop new materials at the nanoscale (in the size range of about 1-100 nm). Their controlled and precise manipulation both at the atomic and molecular level, allows to convey novel properties and features, which can be dramatically different from their corresponding bulk counterparts, i.e., thermal, electrical, mechanical properties. For this reason, in the last decades, the interest in the field of nanotechnology has kept increasing. From an academic point of view, nanotechnological investigations help better understand several phenomena that occur in the gap between atoms and bulk materials. Besides, the vast and versatile library of nanomaterials has the potential to find solutions to several urgent problems related to, e.g., healthcare, energy storage, environment and many others.[1] This can be accomplished also because nanomaterials have witnessed a deep evolution, gaining more and more complexity.[2] Nanomaterials can be divided into different families. Historically, we can distinguish four generations: the first and the second generation consist respectively in passive and active nanostructures. Within the first category, coatings and additives usually used in paints are found. These materials are also used in cosmetic applications. The second generation involves, for instance, electronic devices, sensors, drugs, and chemical delivery systems. The third generation is based on nanosystems in which multiple nanomaterials are assembled to complementarily exploit their properties in the new hybrids. Finally, the fourth generation consists of heterogeneous molecular nanosystems, where every component is engineered to have a specific goal.[2] Nanomaterials can be also classified according to their physicochemical properties or the most abundant element within their structures. In this framework, carbon-based nanomaterials (CNMs) have attracted the attention of the scientific community due to their features and diversity. Indeed, CNMs show a wide heterogeneity in structure, morphology, and physicochemical properties.[3] In the present Feature Article, we will focus on this broad family of nanomaterials and the introduction of amino groups onto their surface. In this context, a strong emphasis will be given on the multiple applications of these newly prepared amino-functionalized CNMs.

1.1. Carbon nanomaterials

Carbon-based nanomaterials (CNMs) have played a major role in the field of nanotechnology. Indeed, the discovery of fullerenes in 1985 represented a breakthrough in the study of nanomaterials. Fullerenes, the first molecular carbon allotrope,[4] are deeply different from other allotropic forms of carbon, namely graphite and diamond. Indeed, C_{60} is the first molecular CNM made only of a discreet number of carbon atoms. After the identification of fullerenes, new carbon-based nanoforms have been welcomed in the CNMs family: from carbon nanotubes (CNTs)[5,6] to graphene;[7] and, more recently, with the advent of carbon dots (CDs).[8] The aforementioned CNMs are the most common, though more exotic nanoforms can be considered too, from carbon nano-onions to carbon nanohorns, nanocones, and nanodiamonds.[3] During recent years, CNMs have gained the limelight of the scientific scene due to their interesting physicochemical properties. However, a major drawback of CNMs in their pristine form is their difficult manipulation and strong tendency to aggregation in most common solvents.[9] Importantly, the features of these carbon-based nanostructures can be easily designed and fine-tuned through the chemical functionalization of their surfaces, improving their solubility and allowing their employment in different technological applications. Chemical functionalization

is also important to alleviate the potential toxicity of CNMs. We demonstrated, in fact, that pulmonary toxicity of pristine, long CNTs can be lifted by suitable functionalization, which allows disentangling of the long ropes and improves dispersibility in water and biological media.[10]

It is worth to mention that every CNM presents a different chemical reactivity based especially, though not only, on the pyramidalization degree of their sp^2 carbon atoms.[11,12] In general, the reactivity is dependent on the curvature of the carbon nanostructure: the more is the surface curved, the more is the system prone towards addition reactions. A separate comment is reserved to graphene, whose edges are usually considered relatively reactive sites.[13] However, the scale of reactivity takes into consideration fullerenes as the more reactive, followed by CNTs and then graphene.

Our group has dedicated its main efforts in the chemical functionalization of the carbon nanoforms, with the scope of transforming CNMs into species resembling simpler organic derivatives. In doing this, the creation of moieties including a pendant amino group has been one of the keys towards the preparation of novel functional materials, aiming at practical applications (Figure 1).

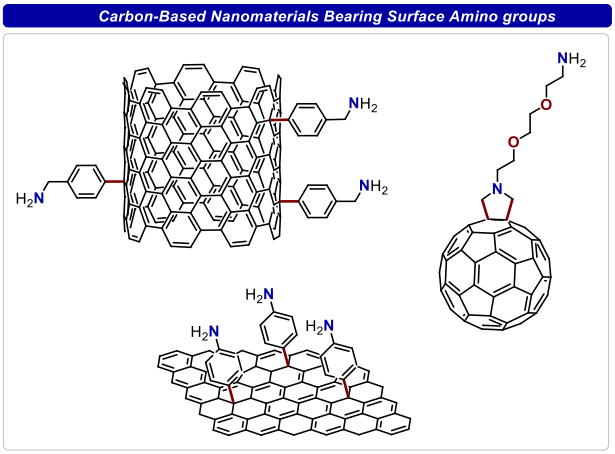

Figure 1: Chemical structures of valuable CNMs bearing surface amino groups. These structures represent very useful intermediates for the preparation of more complex systems.

The first transformation of fullerene into fulleropyrrolidine was carried out in our group nearly thirty years ago.[14] The functionalization of fullerene has paved the way to a multitude of amino-functionalized CNMs. In the present Feature Article, the attention will be focused on the strategies developed in our group for the introduction of amino groups in CNMs and the use of this group for the preparation of highly engineered *ad hoc* nanostructures for practical applications.

2. Importance of amino groups to convey new properties to nanostructures

The covalent functionalization of CNMs is based on the introduction of new chemical groups on their surface *via* common chemical reactions. In particular, the introduction of amino groups is one of the best trade-offs for the preparation of functionalized nanomaterials. Although other kinds of functional moieties can be introduced on carbon nanostructures, e.g., carboxylic acid groups, amine chemistry has outmatched all of them thanks to a series of benefits they can confer to the material. Amino groups are highly versatile chemical functionalities, known for their peculiar electronic and physical characteristics, which deeply impact their chemical properties. The electron-donating properties of amine derivatives lead to the formation of metal complexes with amino-functionalized CNMs.[15] The nitrogen lone pair allows amines to have supramolecular interactions, forming hydrogen and halogen bonds: this property is convenient in the field of sensing and catalysis.[16,17] Amino groups can undergo several chemical transformations due to their nucleophilic nature. This feature can be exploited for reactions with various electrophilic moieties, including aldehydes, acyl halides, and iso(thio)cyanates. Moreover, reaction with carboxylic acids can be used to form amide bonds. All these reactions are of pivotal importance for the connection of CNMs with relevant biomolecules, like peptides and proteins, fluorescent moieties and pharmaceutical drugs.[18,19] Moreover, protective groups – i.e. *tert*-butyloxycarbonyl (Boc), phthalimide (Pht) and many others – can be introduced on amines to prevent their reaction with other susceptible functional moieties. This approach is particularly useful in multistep syntheses and the development of nanomaterials with different types of functionalities.[20] Another property of amines is their intrinsic basicity, which makes them protonated and effectively charged at acidic and neutral pHs. Stable positive charges (quaternary ammonium cations) on the surface of CNMs can be achieved *via* nucleophilic substitution with alkyl halides. The charge complementarity is an effective method for the conjugation with other molecular entities *via* supramolecular interaction.[21] In any case, ammonium cations are well-known for enhancing the dispersion and solubilization of these CNMs in aqueous media, leading to easier manipulation and processibility.[9]

2.1. Quantification of nanomaterial-bound amino groups

For the purpose of this Feature Article, it is convenient to recall the techniques generally employed for the characterization of CNMs and in particular those used for the identification and quantification of amino groups onto their surface. To this end, various approaches can be used, frequently in combination with other strategies. Spectroscopic techniques are always preferred, but direct evidence of successful functionalization with amino groups might not be as simple. Of course, each strategy suffers some limitations. Nuclear Magnetic Resonance (NMR) is a functional technique routinely used in every chemistry laboratory. However, NMR spectroscopy often presents some limitations when analyzing nanomaterials, especially due to their poor solubility in any solvents and to their non-homogeneous nature.[22] To obtain detailed information on the functionalization of CNMs other spectroscopic techniques can be used . Among them, Raman spectroscopy, X-ray photoelectron spectroscopy (XPS), UV-Vis and infrared spectroscopy (IR) are often employed. Raman spectroscopy is a powerful tool for the characterization of CNTs and graphene. This technique allows to obtain structural information about

these materials. Their Raman spectra present three characteristic bands: D band (~ 1350 cm^{-1}, associated with carbon atoms with sp^3 hybridization, meaning defects), G band (~ 1580 cm^{-1}, associated with carbon atoms with sp^2 hybridization) and 2D band (~ 2500-2900 cm^{-1}). The ratio of the D and G band intensities (I_D/I_G) allows to estimate the number of defects present in the materials, and therefore to determine if their covalent functionalization has taken place successfully.[23] XPS is also a useful technique to determine and quantify the elemental composition of CNMs. The emission of photoelectrons, with different intensities and binding energies, from the sample surface allows to obtain information about its chemical composition.[24] Besides, UV-Vis and IR spectroscopies are valuable techniques used to confirm the derivatization of CNMs if the functional groups introduced present characteristic bands. However, these spectroscopic analyses typically provide qualitative information.[25] On the other hand, microscopy techniques enable to observe if the covalent functionalization of CNMs lead to considerable modification of their morphology (e.g. dimensions, aggregation state and functionalization with contrast marker agents).[26] Thermogravimetric analysis (TGA) is also a very useful tool for the quantification of the functionalization degree of CNMs. Other methodologies for the identification and detection of amino groups take advantage of their reactivity. This is, unfortunately, highly dependent on the kind of amine. The simplest strategy for the quantification of amino groups would be an acid-base titration.[27] Of course this case is not practicable, especially in the presence of other basic functional groups. In the best scenario, the detection of amines is subjected to the formation of colored derivatives that can be identified *via* spectrophotometric analysis, namely the reaction with 4-nitrobenzaldehyde,[28] *N*-hydroxy-phthalimide[29] or ninhydrin. A variant of the reaction with the latter reagent is often known as the Kaiser test. Kaiser test is a commercially available analysis kit, routinely performed during the synthesis of peptides. It is carried out by the addition of three different solutions (ninhydrin in ethanol, phenol in ethanol, and KCN in pyridine) to a small portion of the sample. The mixture is heated at 100°C for 5 minutes to afford a colored product known as Ruhemann's purple.[30] This test is selective for the detection of primary amines with at least one proton on the α carbon atom. The molecular structure of the reaction product is independent on the starting amine, allowing a reliable quantification. However, it should be noticed that some amino acids (i.e. proline, asparagine, aspartic acid or serine) do not provide a clear result.[31] As extensively reported by our group, the Kaiser test can be reliably performed for the detection of amines onto nanostructures, particularly for CNMs.[20,32,33] However, this test has some restrictions too, because hindered amines attached onto nanomaterials may not be detected, due to matrix effects. Therefore, the Kaiser test should be considered as a semi-quantitative test, due to its selectivity for primary amines and for the presence of matrix effects, leading to underestimation of the total number of amines.

2.2. Fullerenes

Fullerenes are members of the family of carbon allotropes, which were discovered by Kroto *et al.* in 1985.[4] The smallest fullerene analogue is C_{60}, constituted solely by 60 sp^2-hybridized carbon atoms arranged in a soccer-like spherical shape. The carbon atoms form a truncated icosahedron, composed of 60 vertices and 32 faces, 20 of which are hexagonal and 12 pentagonal (Figure 2). Fullerenes were serendipitously discovered while performing the laser-assisted vaporization of a rotating graphite disk under high helium pressure.[4] Although they were first synthesized in an artificial setup, fullerenes were later found to be naturally occurring in minerals[34] and also in outer space.[35] Higher homologues, like C_{70}, C_{80} and others are also known and widely studied.[36]

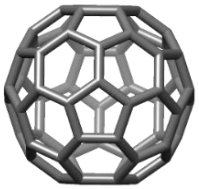

Figure 2: Depictive model for the chemical structure of C_{60}.

2.2.1. Synthetic pathways for fullerene functionalization with amino groups

Since their discovery, fullerenes have had a strong impact on chemistry, physics and materials science, owing to their unique properties.[37] Originally, the biological applications of these carbon nanostructures was difficult, due to their intrinsic poor solubility in aqueous media. In this context, their derivatization with amino groups represented a major breakthrough for their exploitation, allowing also to convey new and unprecedented features to this substrate.[38] One example of functionalization of C_{60} with amino groups was reported by our group in 1993, when the 1,3-dipolar cycloaddition of azomethine ylides, already used for the reaction with olefins,[39] was successfully transferred to C_{60}.[14] In this work, sarcosine was allowed to react with formaldehyde to produce an iminium ion intermediate that, upon thermal decarboxylation, led to the formation of the reactive azomethine ylide **Ia**. Its reaction with C_{60} yielded fulleropyrrolidine **1a** in good yield (41%, 82% based on C_{60} conversion, Figure 3a). Remarkably, a wide variety of fullerene derivatives with the general structure of **1** (Figure 3a, light blue box) can be easily obtained through the rational choice of the amino acids and carbonyl compounds (aldehydes or ketones), showing both the versatility and robustness of this approach.[33,35] Besides, by the appropriate fine-tuning of the reaction conditions, it is also possible to obtain amino-functionalized *bi*- and *poly*-adducts.[41,42] Higher C_{60} homologues (e.g., C_{70}) can be effectively derivatized by this methodology.[43] Later, in 2006, this addition was found to be thermally reversible. Indeed, in the presence of a strong dipolarophile like *N*-phenylmaleimide and a metal catalyst like Wilkinson's catalyst, pristine C_{60} can be obtained from substituted fulleropyrrolidines upon cycloelimination of the pyrrolidine moiety.[44] The retrocycloaddition of azomethine ylides was found to be facilitated by the use of ionic liquids also in the absence of a metallic catalyst.[45]

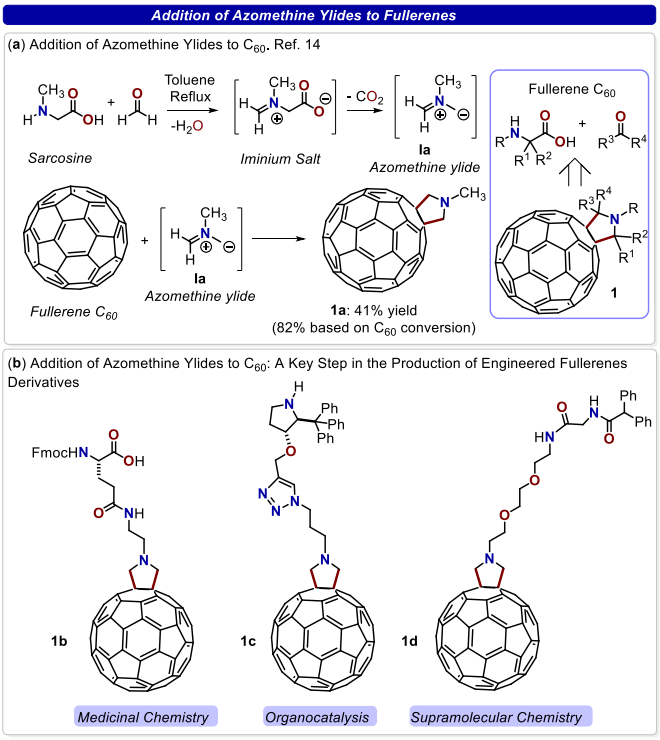

Figure 3: a) schematic representation of the azomethine ylide 1,3-dipolar cycloaddition on C_{60}, general structure of a fulleropyrrolidine monoadduct (light blue box); **b**) some notable fulleropyrrolidines derivatives. Fmoc: Fluorenylmethyloxycarbonyl protecting group.

Optically pure chiral fulleropyrrolidines and fulleroprolines were prepared and characterized through circular dichroism (CD) spectroscopy.[46,47] Owing to the presence of a Cotton effect in the CD spectra, it was possible to assign the absolute configuration to the fullerene derivatives.

In 2009, the possibility to control the stereochemistry of functionalized fulleropyrrolidine was demonstrated. It was achieved *via* metal-catalyzed 1,3-dipolar cycloaddition, allowing the authors to achieve remarkable control of the stereochemical outcome of the reaction.[48] This approach represented a breakthrough for the development of numerous catalytic protocols for the enantioselective functionalization of fullerenes, thus leading to the production of a wide variety of chiral fullerene derivatives with high site and regioselectivity.[49–53] These optically active materials have found applications in fields where chirality is an essential aspect, such as medicinal chemistry and nanobiotechnology.[54] During the course of the years, several other methods have been reported for the derivatization of fullerenes, affording derivatives with the general structure of **1**, such as the photochemical reaction of tertiary amines with C_{60},[55] the desililation of trimethylsilylamino derivatives by thermal or acid-catalyzed mechanisms[56,57] and the ring-opening of aziridines,[14] among others.[58] Another notable example of fullerene derivatization, which allows the successive introduction of amino groups, is the Bingel-Hirsch reaction. This reaction involves a malonate derivative in the presence of a base and carbon tetrabromide (CBr_4) in toluene to afford substituted methanofullerenes.[59]

Usually, most of the aforementioned reactions are carried out in toluene or benzene, which are apolar and toxic solvents used to effectively solubilize fullerenes. Alternatively, the exploitation of ionic liquids (ILs) as reaction media may be considered as a convenient and eco-friendly alternative to these solvents. Indeed, in 2009, our group studied the effect of ILs on the cycloaddition of azomethine ylides (**I**) to C_{60} in combination with microwave (MW) irradiation. In a 3:1 mixture of *o*-dichlorobenzene (*o*-DCB) and 1-methyl-3-*n*-octyl imidazolium tetrafluoroborate, fulleropyrrolidine derivatives can be obtained in less than ten minutes with a conversion up to 98%.[60] It is worth to mention that it is possible to produce selectively either *mono*- or *poly*-adducts by the proper tuning of C_{60} concentration. Interestingly, in bare ILs the reaction does not proceed, due to the high polar nature of these media. Moreover, this feature of ILs can facilitate the retrocycloaddition of fulleropyrrolidine (**1**) to C_{60}, as it was mention previously.[45] Under these conditions, the retrocycloaddition is fast and clean and works with a variety of fulleropyrrolidines.

The presence of amino groups covalently linked to fullerenes allows to exploit their chemistry for further functionalization and subsequent applications. In addition, alkylation of the pyrrolidine nitrogen can be achieved, affording the corresponding fulleropyrrolidinium salts, though the nitrogen in fulleropyrrolidines is less basic and less reactive.[61] This synthetic strategy has been widely used for the modulation of the electrochemical properties[62–64] and the solubility of these nanostructures.[65]

2.2.2. Applications of amino-functionalized C_{60} derivatives

The abovementioned synthetic strategies have allowed many research groups to functionalize C_{60} in many different ways and enabling its use in a wide range of applications. For instance we have shown how C_{60} could be introduced in the lateral chain of an α-amino acid, resulting in the non-natural amino acid **1b** (Figure 3b). The product was obtained by condensation of the terminal amino group, introduced on the C_{60} with the 1,3-dipolar cycloaddition of azomethine ylide, with *N*-Fmoc-L-glutamic acid *tert*-butyl ester.[66] The resulting non-natural amino acid **1b** was then incorporated in peptides *via* solid-phase synthesis.[67] These non-natural peptides were characterized by a good antimicrobial activity, with selectivity towards the Gram-positive bacteria *S. Aureus* and with a minimal inhibiting concentration (MIC) as low as 8-16 μM, albeit a residual hemolytic activity was observed. This antimicrobial activity has been attributed to an increased ability of these synthetic peptides to interact with the cytoplasmatic membrane of Gram-positive bacteria conferred by the fullerene moiety. The introduction of amino groups in its structure provided fullerene C_{60} with novel and unprecedented properties, among them, solubility in aqueous media (up to 10^{-2} M in some examples)[68] that enabled its use in fields like medicinal chemistry. As an example, the anti-HIV (human immunodeficiency virus) properties of the C_{60} scaffold were already known. The pioneering studies in the field, carried out by Wudl and Friedman, demonstrated how the viral protease can be effectively inhibited, thus resulting in antiviral activity.[69] Further investigations on this topic carried out by our group resulted in

a study where we described the synthesis of *di*-cationic fullerenes, obtained by alkylation of the pyrrolidine nitrogen of fulleropyrrolidine *bis*-adducts with methyl iodide. The corresponding pyrrolidinium salts used in this work enlightened how the regiochemistry of these derivatives influences not only their activity as HIV protease inhibitors with high CC_{50}/EC_{50} ratios, but also how it confers selectivity between two different strains of HIV, namely HIV-1 and HIV-2. Moreover, the *trans*-4 stereoisomer was observed to have a five-fold increase in activity against HIV-1 protease compared to the other isomers.[70] The same cationic *bis*-*N*,*N*-dimethylfulleropyrrolidinium salts were also studied as inhibitors of the acetylcholinesterase enzyme. Both computational and experimental studies evidenced how C_{60} can fit in the active pocket of the enzyme. The inhibition of the enzyme was a non-competitive process with affinity constants in the micromolar range, making these cationic fullerene derivatives interesting candidates also for the modulation of acetylcholinesterase activity.[71] Polycationic fullerene derivatives were also evaluated as gene transfection agents, as shown by the pioneering work reported by Nakamura *et al.* This group synthesized a *di*-cationic fullerene and studied its ability to interact with deoxyribonucleic acid (DNA) and to act as a carrier to mediate cell internalization. The application of this fullerene derivative was however hampered by solubility issues, polar and toxic solvents like dimethylsulfoxide (DMSO) and *N*,*N*-dimethylformamide (DMF) had to be added to help the solubilization of the carrier.[72] This concept was further developed by us, when we carried out the synthesis of a polycationic fullerene derivative. This derivative showed a strong interaction with plasmid DNA with an association constant of 7.74×10^8 M^{-1} and good results in cellular uptake tests.[73]

Amino-derivatized fullerenes have also been used in several applications belonging to other research fields like catalysis.[74] A chiral amino-functionalized C_{60} was used for instance as π-acid catalyst for the Diels-Alder reaction between hydroxypyrone and maleimide derivatives in deuterated chloroform ($CDCl_3$), achieving good diastereoselectivity between the *exo/endo* products (ratio of *exo/endo* = 0.56 with 55% enantiomeric excess of the *exo* product).[75] In another example of asymmetric organocatalytic transformation, the optically active fullerene-trityl pyrrolidine hybrid **1c** (Figure 3b) was used for the asymmetric addition between derivatives of dimethyl malonate and cinnamaldehyde with an excellent conversion (up to 90% yield) and enantioselectivity (up to 94%). The recyclability of this catalyst, conferred mostly by the fullerene moiety, was also demonstrated. After six catalytic cycles, only a minor loss of catalytic performance was observed, with unaltered enantioselectivity.[76]

Many applications of fullerenes functionalized with the 1,3-dipolar cycloaddition in energy related fields have been reported, mainly because of the excellent optoelectronic properties of the carbon sphere.[77] C_{60} has a favorable band-gap (2.3 eV in the solid state) and an *n*-type material character:[78] because of these features this scaffold was extensively used in the fabrication of photovoltaic devices.[79] Guldi *et al.* reported the synthesis of a tetrafullerene array, in which *N*-octyl functionalized fulleropyrrolidines are linked by a π-conjugated light-absorbing oligomeric central core.[80] By blending this material with poly(3-hexylthiophene) in a 1:1 ratio they were able to fabricate a glass supported device with an external quantum efficiency of 15%. In another example, a cationic fullerene was instead used to form a supramolecular adduct *via* electrostatic interactions at the air-water interface of a Langmuir film with negatively charged, water-soluble carbon dots (CDs), a carbon nanomaterial that we will discuss more in detail in section 2.5. This film was transferred on an indium doped tin oxide glass (ITO) substrate by using the Langmuir-Schaefer method[81] and the performances of the so obtained device were tested. Although the devices showed a low short circuit current (21.8 μA/cm) and incident photon to current efficiency (IPCE) of 0.35%, this represents a proof of concept that opens relevant perspectives in the fabrication of all-organic solar energy conversion systems based on the interaction between two different carbon nanomaterials.[82] This last example clearly indicates how achieving a supramolecular control of the spatial arrangement of the components in a system is a key aspect to fine-tune its characteristics.

Fullerenes were also found to be a very interesting scaffold in supramolecular chemistry.[83] In this context, we have reported how dibenzylammonium functionalized fullerenes, obtained through the Bingel protocol, can form [2]- and [3]-pseudorotaxanes with dibenzo-[24]-crown-8-ether derivatized porphyrins. Interestingly, the supramolecular assemblies showed enhanced third-order non-linear optical properties (NLO) compared to the sum of those of the separate components. These emerging features can be modulated by the variation of the protonation state of the dibenzylammonium recognition site upon the addition of a base, allowing to switch the system between two "on-off" states.[84]

Because of its intrinsic bulkiness, fullerene is an ideal stopper unit for the synthesis of mechanically interlocked molecules (MIMs).[85] We have synthesized several rotaxanes containing C_{60} as stoppering unit. In this work, we have synthesized axle **1d** (Figure 3b), consisting of a fulleropyrrolidine bearing a glycolic chain with a terminal amino group that was condensed *via* an amidation reaction with diphenylacetylglycine, which represents the other stoppering unit. The resulting interlocked structure, obtained with this axle and a ferrocene functionalized macrocycle, exhibited a *stimuli*-responsive bistable behavior, allowing the modulation of the photoinduced electron transfer between fullerene and ferrocene.[86] In a similar rotaxane, but without the ferrocenyl moieties, the position of the macrocycle is capable to allosterically induce a selectivity in the position of introduction of a second pyrrolidinic group, resulting from a second cycloaddition to the fullerene stopper.[87]

2.3. Carbon nanotubes (CNTs)

Carbon nanotubes (CNTs) can be considered rolled graphitic sheets forming cylinders with lengths of micrometers and diameters up to 100 nm. These carbon nanostructures can be classified in single-walled carbon nanotubes (SWCNTs) and multi-walled carbon nanotubes (MWCNTs), depending on the number of concentric tubes that compose the material (Figure

4).[5,6,88] It is worth to mention that in the case of SWCNTs, their electrical properties are determined by the way the graphitic sheet is rolled up. Depending on the arrangement of the hexagonal rings along the tubular surface, these CNTs can be metallic or semiconducting.[89] Due to their extraordinary mechanical, electrical and thermal features,[90] CNTs have been employed in several nanotechnological applications, such as fillers in polymer matrixes, solar and fuel cells and (bio)sensors, among others.[90–92] However, one of the major drawbacks of CNTs is the formation of aggregates or bundles as a consequence of their intertube forces, making difficult their suspension in solvents and their manipulation for diverse purposes. To overcome this problem, the surface modification of CNTs is necessary, exploiting their chemical derivatization by distinct methodologies.[93,94]

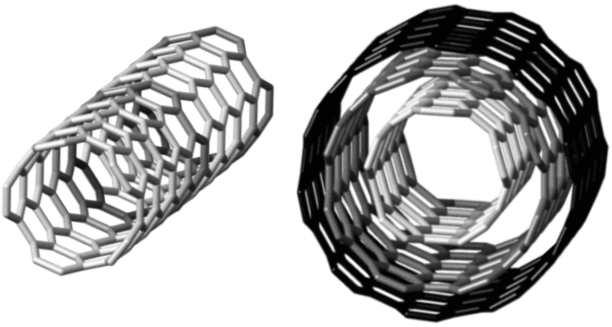

Figure 4: Depictive models for the chemical structure of SWCNT (left) and MWCNT (right).

2.3.1. Synthetic pathways for CNTs functionalization with amino groups

The covalent functionalization of CNTs by a few organic reactions improves the dispersion in several solvents and allows the attachment of diverse functional groups, especially amino groups. In 2001, Tour *and coll.* developed a novel and efficient method for the functionalization of small-diameter SWCNTs (**2**, ca. 0.7 nm) exploiting the reactivity of aryl diazonium salts (Figure 5a).[95] The diazonium salts employed in the modification of pristine SWCNTs (*p*-SWCNTs) were synthesized from the corresponding aniline derivatives using nitrosonium tetrafluoroborate ($NOBF_4$). The reaction of the aryl radicals (**II**), formed by the electrochemical reduction of the aryl diazonium salts, with the surface of the SWCNTs produced the functionalized materials **3** (*f*-SWCNTs). The same group has found that this approach works also when *p*-SWCNTs are directly treated with the aryl diazonium salts under moderate thermal conditions[96] or when the diazonium species are generated in situ (Figure 5b and 5c).[97,98] In all cases, the functionalization degree seems to depend on the nature of the *para*-substituent (R) of the aniline derivative.

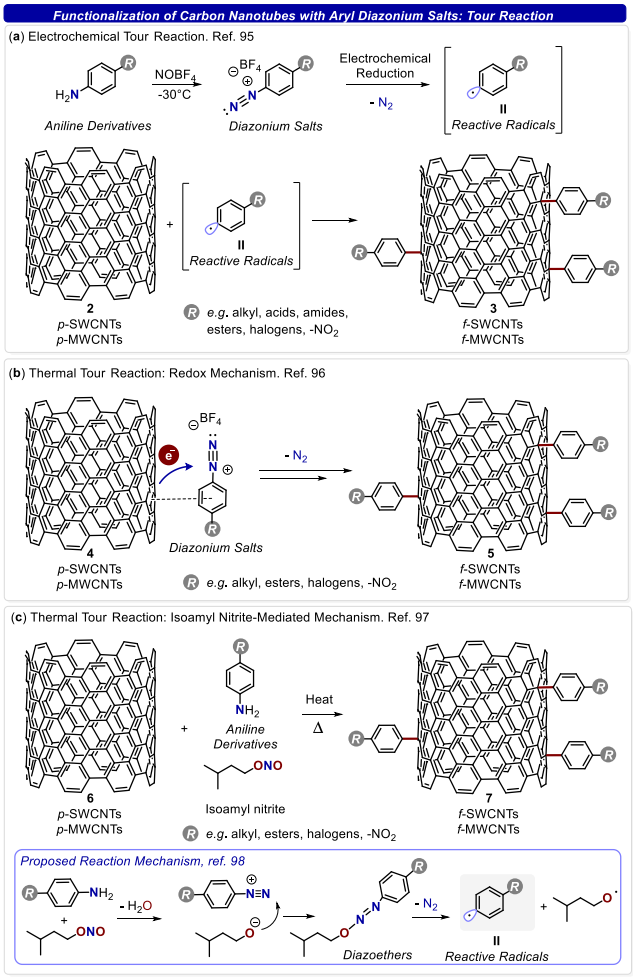

Figure 5: Different approaches to the arylation reaction on CNTs.

In 2002, our group reported a versatile functionalization method based on the 1,3-dipolar cycloaddition of azomethine ylides (**I**), generated in situ by the condensation of α-amino acids and aldehydes.[99] The obtained *f*-CNTs **9** were suspendable in most organic solvents, such as chloroform, acetone, tetrahydrofuran (THF), and even in water (Figure 6). Indeed, utilizing the 1,3-dipolar cycloaddition, *f*-CNTs **9d** and **9e** (Figure 6) can be obtained. The deprotection of the amino groups and the presence of hydrophilic chains allow the dispersion of these CNTs in aqueous media.[100] Moreover, these amino-functionalized CNTs are suitable for subsequent covalent or non-covalent derivatization with many (bio)molecules.[18]

It is worth to mention that making use of these two functionalization approaches (Figure 5 and 6), in principle, any moiety could be attached to the surface of SWCNTs and MWCNTs in an easy way.[101]

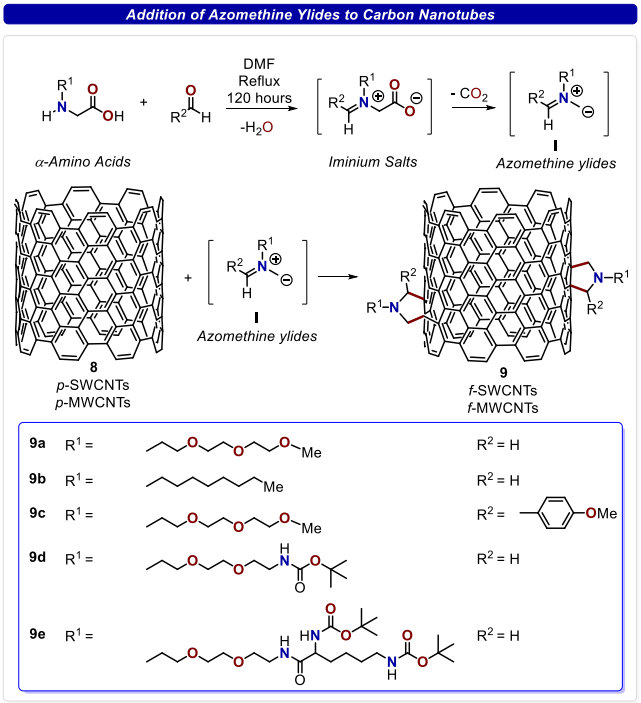

Figure 6: 1,3-dipolar cycloaddition of azomethine ylides to CNTs.

In the attempt to improve the control of the functionalization of CNTs, several alternative approaches have been developed in the past years in order to simplify and scale-up the process. The employment of solvent-free conditions[102] and MW irradiation allows the functionalization of CNTs in shorter times and the scale-up of the reaction.[103] The introduction of more than one functional group by multiple reactions is a powerful tool that may confer several new properties to the materials at the same time.[104–106] In 2008 in order to optimize the double functionalization protocol, we devised a novel synthetic methodology based on the functionalization of CNTs using both the 1,3-dipolar cycloaddition of azomethine ylides and the radical addition of diazonium salts.[107] In this approach, both treatments occur *via* a simple and fast MW-induced method that allows reducing the reaction times with respect to the original conditions.[99,108] We also observed that the change in the order of reactions influences the functionalization degree of the 1,3-dipolar cycloaddition. This observation permits the control of the quantity of different functional groups attached to the surface of CNTs. Following this concept of multi-functionalization strategy, the attachment of three different active groups in one step employing the arylation reaction was reported in 2011 (Figure 7).[20] The presence of three different protecting groups in the benzylamine moieties allows their specific and sequential removal. This approach allows to bind three different molecules of interest in a controlled manner on the surface of CNTs.

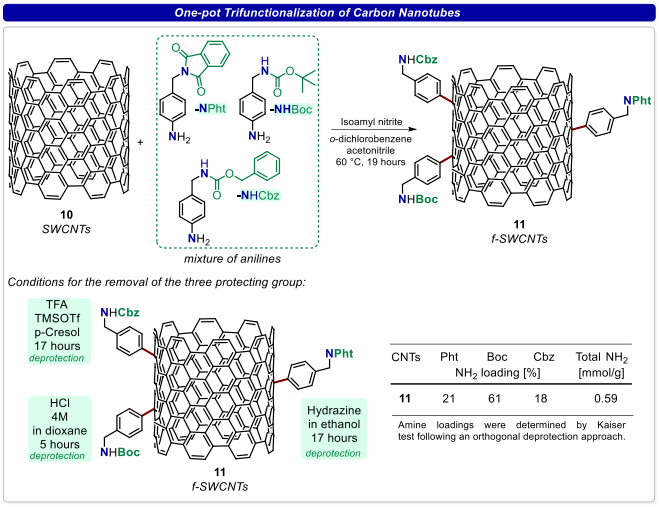

Figure 7: One-pot triple functionalization of CNTs.

Other versatile and reliable methods for the covalent functionalization of CNTs have been reported. One notable example, reported by Tour *et al*, is their functionalization employing ILs as reaction medium.[109] In 2005, they showed that grinding SWCNTs with a variety of diazonium salts, in the presence of a base, afforded *f*-CNTs. Following this approach, we studied the effect of ILs on the functionalization of SWCNTs in combination with MW irradiation. In contrast with the observations made by using C_{60} as a substrate, we found out that the cycloaddition of azomethine ylides to CNTs can be carried out in bare IL, yielding from good to excellent functionalization degrees.[60] In addition, also in this case, we have observed that the use of *o*-DCB as co-solvent highly improves the derivatization of SWCNTs. Within this context, we have also studied how ILs impact on the functionalization degree of this material, thus exploring different reaction conditions.[110] Remarkably, ILs along with MW irradiation favor the high surface functionalization of SWCNTs at short reaction times, but hamper it at longer times. In both cases, the *f*-CNTs were characterized *via* Raman spectroscopy and thermogravimetric analysis. Another example is the functionalization of CNTs with disulfide derivatives (aliphatic and aromatic) allowing the introduction of different amino moieties.[111,112] The reaction occurs under an inert atmosphere at reflux in toluene for 48 hours. A possible initial stage for the reaction could be the homolytic cleavage of the weak sulfur-sulfur bond. The resulting thiyl radicals then would attack the surface of CNTs.

2.3.2. Applications of amino-functionalized CNTs derivatives

The major difficulty in the integration of these nanostructures into biological systems was their poor solubility in aqueous media. The employment of the azomethine ylide 1,3-dipolar cycloaddition reaction allows the functionalization of CNTs with free amino groups that improve their dispersion in water, as mention above. These amino groups can be modified with several biomolecules,[100] e.g., leading to delivery systems of different therapeutic agents such as peptides,[19,113] nucleic acids (nucleotides, DNA or RNA)[18,114–117] or small molecules

(anticancer, antibacterial or antiviral agents).[118,119] As an example, in 2005, making use of the double functionalization strategy, a fluorescent probe (fluorescein) and an antibiotic moiety (amphotericin B) were linked to MWCNTs, after the selective removal of two different protective groups (Figure 8).[120] Cell uptake of *f*-MWCNTs **12** was confirmed by epifluorescence and confocal microscopy. Furthermore, it was observed that the toxic effects of amphotericin B on mammalian cells were reduced when the drug was bonded to MWCNTs, while its high antifungal activity was preserved.

Due to their electrical conductivity, mechanical strength, and flexibility, CNTs are promising materials for the interaction with electrically active tissues, such as neuronal and cardiac tissues. Indeed, pristine CNTs have been employed as two-dimensional (2D) scaffolds for the growth of neuronal networks and cardiomyocytes.[121,122] Both types of cells grown onto these scaffolds present an increase in their electrical activity.

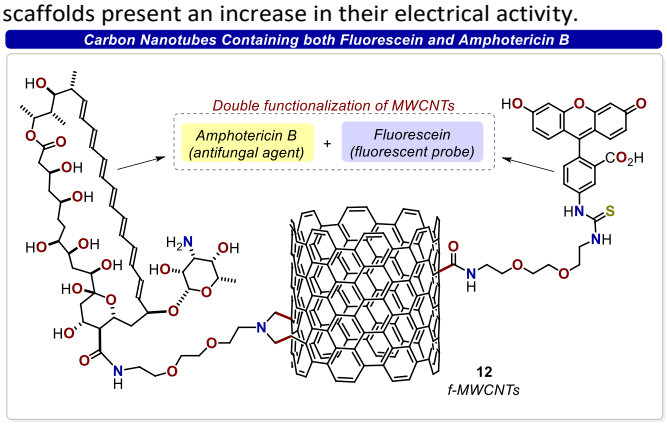

Figure 8: Double functionalized MWCNTs with a fluorescent probe and an antifungal agent.

Focusing on the case of neurons, we investigated how the functionalization of CNTs modifies the ability of the 2D scaffolds to boost neuronal growth and communication. For this purpose, in 2016, MWCNTs were functionalized employing the 1,3-dipolar cycloaddition of azomethine ylides and the arylation with diazonium salts.[123] It was observed that, both the functionalization degree and the nature of the side chain attached to the surface of MWCNTs affect the electronic properties of the scaffolds and therefore modify the synaptic activity of neuronal cells. More extensive functionalization degrees compromise the interneuronal communication, which is kept intact in the case of light functionalization degrees.

The construction of 3D scaffolds allows to mimic the complexity of the neuronal and cardiac tissues and to study how the 3D morphology affects the growth and activity of these cells. We developed a micro-porous, self-standing, elastomeric scaffold made by polydimethylsiloxane, in which CNTs are entrapped.[124] In the case of neurons, the 3D scaffold further improved the efficiency of neurons and neuronal connections with the synchronization of their activity. In the case of cardiomyocytes, their viability, proliferation, and maturation were enhanced by the 3D scaffold.[125]

The functionalization of CNTs allows the development of 3D scaffolds as injectable gels for cardiac tissue engineering perspectives. Also, in this case, the viability, proliferation, and maturation of cardiomyocytes were improved.[126]

The functionalization of MWCNTs with the Gd^{3+} chelating agent diethylene triamine pentaacetic acid (DTPA) and the subsequent formation of the Gd-MWCNTs conjugate yields very stable and efficient platforms for Magnetic Resonance Imaging cellular probes, with a relaxivity of 6.61 $s^{-1}mM^{-1}$, that is not quenched when Gd-MWCNTs are internalized by the cells employed in the study. This result is a significant advantage over other Gd-based nanoparticles, where a strong quenching is observed.[127]

The molecular recognition of flavins (cofactors of flavoproteins and active sites in redox catalytic processes) by a receptor is important in the development of sensors and also in the improvement of chemical models to understand the role of the non-covalent interactions in enzymatic processes. In this regard, CNTs have been modified with two different functional groups (*p*-tolyl and triazine) using the radical addition of aryl diazonium salts, with the aim to study the differences in the interaction with riboflavin between the two motifs.[16] In both cases, the π-π interactions of riboflavin with the walls of CNTs are inhibited by the presence of the functional groups, so the differences between both systems are due to the different kinds of interactions. It was determined that the recognition of riboflavin is better in the case of CNTs functionalized with triazine moieties, due to the ability to form hydrogen bonds. In addition, the results of the electrochemical studies reveal that these *f*-CNTs are promising platforms for the design of flavin receptors.

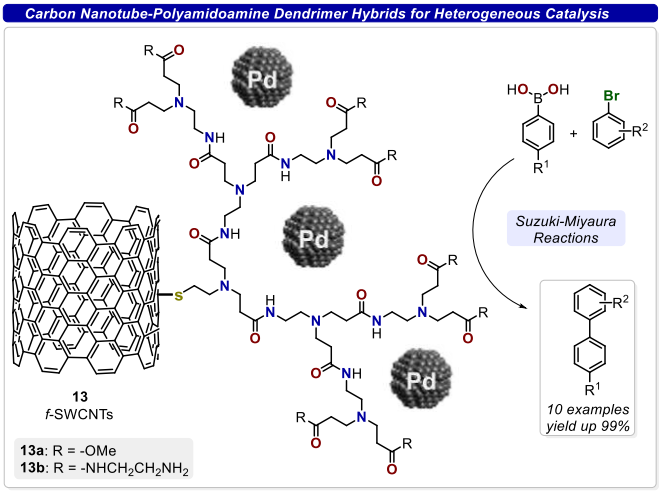

Figure 9: PdNPs-SWCNTs catalysts for C-C cross-coupling reactions.

CNTs are also useful scaffolds in heterogeneous catalysis.[128] Efficient and stable nanostructured oxygen-evolving anodes were developed for efficient water oxidation.[129] These nanostructures are fabricated by the electrostatic interactions between an oxygen-evolving negatively charged polyoxometalate (POM) cluster[130] and positively charged dendron-MWCNTs. These *f*-MWCNTs were synthesized by a series of alkylation reactions between amino-functionalized MWCNTs with glycidyltrimethylammonium chloride, and/or with a mixture of acrylate and ethylenediamine.[116]

CNTs can be also employed as heterogeneous catalysts in organic reactions. We reported an efficient palladium-supported catalyst for Suzuki and Heck reactions (C-C cross-coupling reactions) (Figure 9). In this case, SWCNTs were functionalized with polyamidoamine dendrimers (PAMAM) by the direct reaction between SWCNTs and disulfide derivatives and subsequently, the palladium nanoparticles (PdNPs) were immobilized by an "in situ" strategy.[131] Two different nanomaterials, **13a** and **13b**, with two different sizes of PdNPs were obtained, and it was determined that the SWCNTs loaded with the smaller PdNPs presented better catalytic performances for both coupling reactions. This nanocatalyst presents a high turnover number and turnover frequency and can be recycled up to six times.

2.4. Graphene

Graphene is a monolayer of sp^2 hybridized carbon atoms arranged into a two-dimensional honeycomb structure with dimensions ranging from a few hundred nanometers to tens of micrometers (Figure 10).[7,132]

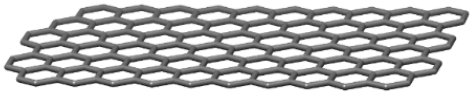

Figure 10: Depictive model for the chemical structure of graphene monolayer.

Different types of graphene-based materials can be defined according to the number of layers, their dimensions, and the amount of oxygen present in the structure.[133] Due to their unique characteristics, graphene materials have been applied in a wide range of fields, such as sensing, energy storage, and optoelectronic devices, among others.[134–137] Graphene is prepared by several methods that can be divided into bottom-up and top-down approaches, depending whether graphene is grown by small molecular precursors (bottom-up) or exfoliated from the bulk graphite (top-down).[132,138] An ideal route to produce graphene monolayers is the growth and deposition of this material on substrates.[139] Among all the methods that allow the production of graphene monolayers, chemical vapor deposition (CVD) is a more promising and economic approach to produce high-quality graphene. However, the employment of expensive transition metal substrates (Pt, Ir, Rh, Ru) and harsh growth conditions (high temperature and high vacuum) are important drawbacks for the scale-up synthesis of graphene.[140] On the other hand, the exfoliation of graphite in liquid media presents several advantages such as its versatility, simplicity, and potential scalability. The obtained dispersions are mixtures of mono and few layers of graphene (FLG) with an overall good quality. Another approach to generate relatively concentrated dispersions of FLG is the employment of ball-milling. In this method, a solid mixture of melamine and graphite is ball-milled, the adsorption of melamine on graphene compensates the strong π-π interactions between layers, allowing the exfoliation of graphite. The solid mixture can be dispersed in DMF or water producing concentrated dispersions of FLG.[141] In addition, the FLG dispersions can be used for graphene composites or films.[142] Considering these two general pathways, the covalent functionalization of the material, in order to modulate its physical and chemical properties, can be carried out in solution/dispersion or on solid surfaces.[13,143]

2.4.1. Synthetic pathways for graphene functionalization with amino groups

Like other CNMs, graphene has tendency to aggregate as a consequence of strong π-π interactions among layers.[138] Moreover, the graphene sheets are hydrophobic, making their dispersion difficult in polar solvents.[144,145] For these reasons, the production and handling of graphene dispersions are technically challenging. Therefore, as in the case of CNTs, the chemical functionalization of graphene is essential to make it dispersible in several solvents and suitable for applications.[146] Since many uses are based on graphene composites or films, and these are easily produced by graphene dispersions, the following examples are going to focus on the functionalization of graphene in liquid media.[147] The first step in the functionalization of graphene in solution is the production of stable dispersions, which can be obtained by exfoliation of graphite in *N*-methylpyrrolidone (NMP), affording a mixture of single and few layers of graphene (FLG).[148] Then, the functionalization can be accomplished by several standard protocols.

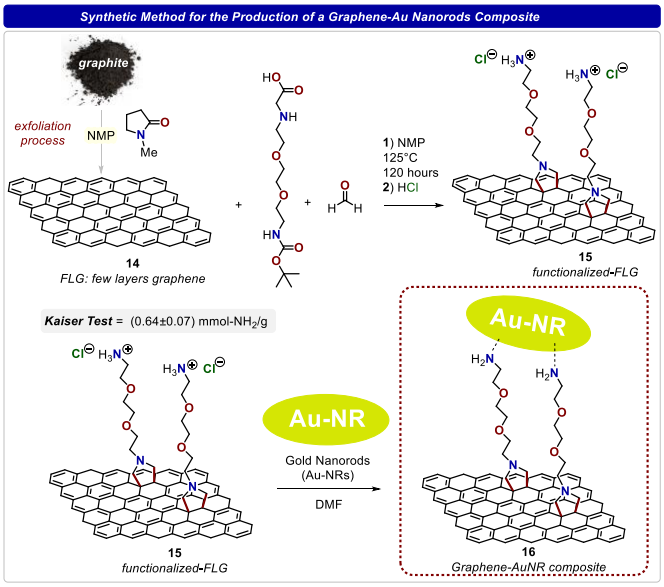

Figure 11: Functionalization of graphene via 1,3-dipolar cycloaddition and production of a graphene-Au nanorods composite.

In our group, we have used the 1,3-dipolar cycloaddition reaction (Figure 11).[32] The deprotection of the Boc group, present in the modified α-amino acid used, allows to verify the presence of free amino groups in the functionalized material (**15**) utilizing the Kaiser test. To localize the functional groups on the graphene layers, gold nanorods (AuNRs) were used as contrast marker agents exploiting their interaction with amines (**16**). The study of this hybrid by transmission electron microscopy (TEM) showed the presence of AuNRs distributed uniformly all over the graphene layers, corroborating the

hypothesis that the 1,3-dipolar cycloaddition reaction occurs also in the central C-C bonds of FLG. The use of gold nanoparticles (AuNPs) as contrast markers allowed to identify the reactive sites of FLG. In this case, the functionalization was carried out by the 1,3-dipolar cycloaddition or by the amide-bond condensation on the carboxylic groups generated during the sonication process for the exfoliation of graphite.[149] In both cases, FLG was functionalized by PAMAM dendrimers (Figure 12). The deprotection of the Boc moieties permitted to quantify the free amino groups present in both functionalized materials, **17** and **18**, being the number of these groups lower in the case of *f*-FLG with the amidation reaction (**18**). In order to determine where the functionalities introduced by the two reactions are located, the formation of the hybrids with AuNPs was performed. As previously discussed, TEM studies determined that the 1,3-dipolar cycloaddition takes place all over the FLG surface. Meanwhile, for the amidation reaction, the AuNPs seem to be deposited mainly at the edges of the layers. This result, together with the values of the Kaiser test are indirect proofs that FLG obtained after the sonication process presents a low concentration of carboxylic groups, which are mostly located at the edges.

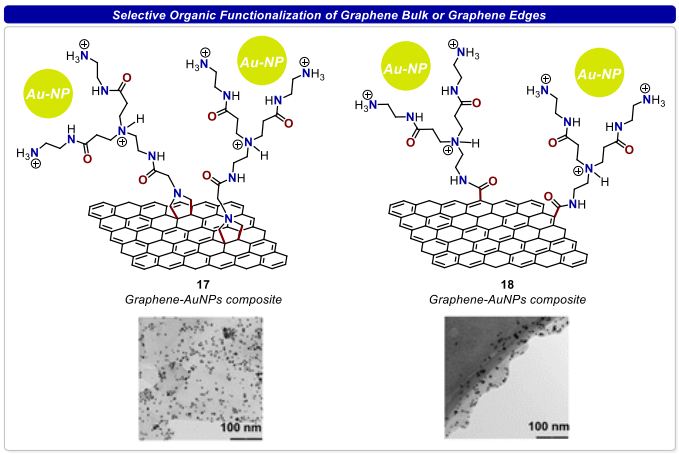

Figure 12: Gold nanoparticles as contrast markers to identify FLG reactive sites. [149] – Adapted by permission of The Royal Society of Chemistry

Another approach for the functionalization of FLG is the addition of aryl diazonium salts.[150,151] This strategy, typically, leads to high functionalization degrees and has also the advantage of being tolerant of a variety of conditions. The presence of free amino groups on the surface of FLG allows the supramolecular interaction of these functionalized materials with other moieties. With the aim to determine which is the best functional group for the interaction of *f*-FLG with polyoxometalate (POM) units, two different substituents (PAMAM or *N,N,N*-trimethylbenzeneammonium) were attached employing the 1,3-dipolar cycloaddition or the radical arylation reaction, then the polyanionic Ru_4POM was captured by the ammonium cations through electrostatic interactions.[152] By means of the aberration-corrected-TEM (AC-TEM), it was possible to study this interaction by a dynamic approach. During the AC-TEM studies, it was observed the dynamic motion of POM units as a consequence of their interaction with the electrons of the incident beam. In order to monitor this movement, a series of images were taken along time. It was observed that the POM units attached to *N,N,N*-trimethylbenzenaminium remain static for a longer time compared with the units attached to PAMAM and also possess a lower degree of motion freedom. These results indicate that a functional anchor of a larger size (PAMAM) allows a more active interaction of POM units with the environment, which is beneficial for catalytic applications.

An alternative functionalization pathway is the employment of graphite intercalation compounds (GICs), which can be dispersed in the form of negatively charged graphene sheets (graphenides, the reduced form of graphene).[153,154] This procedure guarantees a facile reaction with several electrophiles as a consequence of the negative charges present on the graphene layers. Besides, monolayer graphenide sheets are the main species due to strong solvation.[155] In a recent study it was determined that the reactivity of graphenide depends on the solvation of the present counterions. For this purpose, the dispersion and functionalization with GIC were carried out in five different solvents (DMF, NMP, THF, 1,2-dimethoxyethane (DME), and diglyme), in the presence or absence of cation complexing agents (18-crown-6-ether or diglyme) and using 4-iodoaniline and 4-fluorobenzene-diazonium tetrafluoroborate for the covalent modification (Figure 13).

The reaction between graphenides and the organic moieties occurs *via* radical mechanism allowing to obtain functionalized graphene layers, **19** and **20**.[156] The differences between all the reaction conditions were studied by scanning Raman spectroscopy (SRS), examining the ratio between the D band (~ 1340 cm^{-1}) and the G band (~ 1580 cm^{-1}). It was observed that the reactivity of graphenide increases with the solvation ability of potassium cations of the different solvents. Surprisingly, diglyme presents the lower degree of functionalization with a stronger coordinating ability (solvation) towards potassium cations. This is due to the high effective ionic concentration of the dispersion that leads to destabilization and faster aggregation of graphenide flakes, hampering their functionalization. In order to better understand this effect, the functionalization was carried out in the presence of the cation complexing agents, that improve the solubility of cations. It was determined that an excessive solvation leads to destabilization and to a lower reactivity of graphenides, as in the case of diglyme. Therefore, for an efficient functionalization of graphene employing this approach it is necessary to find the appropriate solvation of potassium cations improving the reactivity of graphenide.

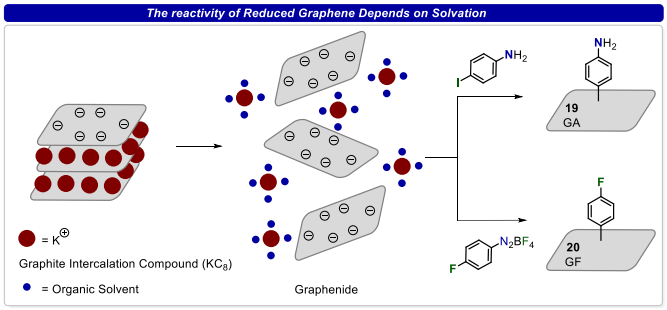

Figure 13: Covalent functionalization of graphene starting by graphite intercalation compounds.

2.4.2. Applications of amino-functionalized graphene derivatives

The functionalization of graphene with various functional groups, especially with amino groups through diverse approaches, allows its interaction with other functional molecules or nanostructures for the subsequent application of these materials in diverse fields. As it was mentioned above, *f*-FLG can interact with different inorganic nanostructures to form scaffolds for composites. The unique electronic, mechanical, and chemical features of graphene turn it into an interesting material as catalyst support.[157] In 2013, a functionalized graphene platform was designed to host a polyanionic POM catalyst, mimicking the oxygen-evolving center of natural photosystems (Figure 14).[158] FLG was functionalized by the 1,3-dipolar cycloaddition and the subsequent condensation reaction for the attachment of PAMAM dendrimers. Then, the POM units were introduced in the structure exploiting the complementary charge attraction between the positive groups located at the graphene surface and the negative POM moieties. It was demonstrated that the graphene platform outperforms the catalytic water oxidation efficiency of the POM units alone or supported on CNTs.[129] Another efficient strategy to modify FLG with POM entities was the functionalization with *N,N,N*-trimethylbenzene ammonium groups employing the radical arylation reaction.[159] As in the previous example, the POM units were immobilized through electrostatic interactions and their catalytic activity was retained. The final hybrid material is able to decompose hydrogen peroxide (H_2O_2) to oxygen, as it was observed when aqueous H_2O_2 was added to graphene hybrid resulting in the expected oxygen evolution.[21]

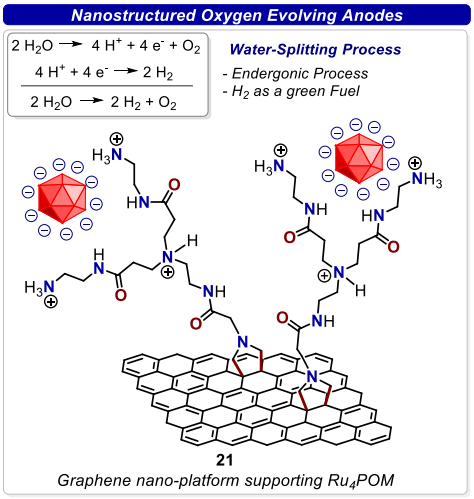

Figure 14: Functionalized FLG with POM units for water oxidation catalysis.

The same characteristics that convert graphene into a fascinating platform for catalysis allow its application in sensing.[135] Recently, a potential sensing platform for carbohydrate-lectin interactions was developed by the chemical functionalization of chemical vapor deposited graphene (CVDG). This platform is based on the preparation of glycan arrays.[160] The first step for the construction of these arrays is the covalent functionalization of graphene surface with stearyl alkoxide-substituted derivative employing the radical arylation reaction, **23**. Then the *N*-hydroxysuccinimide activated bidentate 1,2-*sn*-dipalmitoyl glycerol was incorporated on the graphene surface by hydrophobic interactions, **24**. Onto this activated hydrophobic surface, 5-amine-pentyl modified carbohydrates were immobilized as carbamates (**25**, Figure 15). This complex structure was constructed onto two different substrates (ITO-coated glass and uncoated glass slides). The successful immobilization of the activated glycerol linker and the different carbohydrates was monitored by matrix-assisted laser desorption/ionization time-of-flight (MALDI-TOF) mass spectrometry (MS). Under laser irradiation, the hydrophobic surface is disrupted allowing the detection of carbohydrates. Finally, the detection of carbohydrate-lectin interactions on these microarrays was studied by MS and fluorescence spectroscopy. The CVDG carbohydrate microarrays were incubated with a fluorescent labelled lectin that recognizes specifically the L-fucose motif. Fluorescence was only observed in the spots corresponding to the fucosylated carbohydrate on the array. In addition, after the incubation of the array with this lectin, a peak at m/z = 33691 Da was detected by MALDI-TOF MS exclusively in the spots where the fucosylated carbohydrate was located. These results confirm that this CVDG platform can be exploited in sensing for the study of carbohydrate-lectin interactions and also as a component for MS analysis.

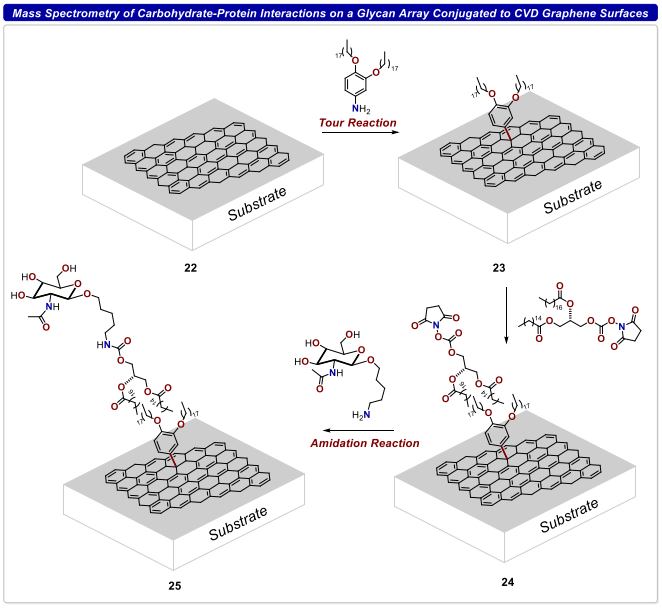

Figure 15: Functionalized CVDG platform for carbohydrate-lectin interactions.

2.5. Carbon dots (CDs)

Carbon dots (CDs) are the latest class of CNMs discovered, consisting of *quasi*-spherical nanoparticles with diameters typically below 10 nm.[161] Their elemental constituents are mainly carbon, hydrogen, and oxygen, but other atoms like nitrogen or sulfur are often encountered.[162] Their discovery dates back to 2004 when, while analysing the production residues of CNTs by arc discharge, Scrivens *et al.* noticed this highly fluorescent and fast-moving material in the electrophoresis plate.[8] Since then, CDs have witnessed an always growing interest from the scientific community, because of their excellent photoluminescent (PL) properties (excitation dependent fluorescent emission), biocompatibility, and low production costs. The aforementioned characteristics make CDs privileged candidates for a vast number of applications. Because of the ambiguous classification that can be encountered in literature, we will adopt, in this context, the classification proposed by Arcudi *et al.*,[163] in which these materials can be divided into two main categories depending on the reaction conditions, where the temperature is a crucial parameter. Temperatures above 300°C usually afford CDs characterized by a graphitic core (*g*-CDs), like graphene quantum dots (GQDs) and carbon quantum dots (CQDs). Below this threshold, materials characterized by an amorphous core (*a*-CDs) are obtained. The optical properties of *g*-CDs are usually associated to the delocalized band structure resulting from the graphitic core. *a*-CDs are instead characterized by a higher content of sp^3 carbon atoms and their photoluminescent behavior is related to molecular-like species.[163] Albeit the PL properties can be ascribed to these two general mechanisms for the sake of simplicity, both effects might contribute to the overall PL features depending on the nature of the material.[164] The mechanisms underlying the formation of both *g*-CDs and *a*-CDs are still under debate in the scientific community, but general hints deriving from the large amount of data on this topic indicate that polymerization and aromatization play a predominant role.[165] Nowadays many synthetic protocols have been developed to obtain CDs, but all of them can be ascribed to two main approaches: top-down and bottom-up methods.[166] The former is achieved by high energy treatment of large carbon structures (e.g., CNTs, amorphous carbon, etc.). Typical protocols include arc discharge,[167] laser ablation,[168] and electrochemical oxidation.[169] The bottom-up methodologies exploit instead the thermal treatment of small molecular precursors and are achieved by solvothermal, MW-assisted, and pyrolytic methods. Both approaches present advantages but, through the bottom-up method, it is possible to employ a wider variety of precursors, achieving a greater control over the resulting material and a fine-tuning of their properties while aiming for a specific application.[163] The materials obtained with bottom-up synthesis are generally derived by solvothermal treatment, due to the versatility and low production costs that this approach offers.[170] Among the hydro- and solvothermal methods, that historically relied on the use of an autoclave and often required long reaction times, the MW-assisted procedures have rapidly emerged as a reference in terms of reaction time, energy consumption, and reproducibility.[33] In the last few years, numerous syntheses of CDs have been reported, and some examples of the wide variety of substrates from which CDs were obtained comprises carbohydrates,[171] amino acids,[172] ethylenediaminetetraacetic acid (EDTA),[173] citric acid[174] and raw materials.[175] Depending on the materials used for the synthesis and the heteroatoms present in their structure, several different functional groups can be obtained on the surface of the resulting material.

2.5.1. Bottom-up pathways for amino-functionalized CDs

Indeed, the possibility of the introduction of heteroatoms significantly widens the range of possible CDs that can be obtained.[176] Doping with heteroatoms dramatically influences the properties of the final material and N, O, P, B, and S are the elements most frequently reported for the doping.[177] Materials obtained by nitrogen doping, that we will refer to as nitrogen-doped carbon dots (*N*-CDs), show very interesting characteristics. They are usually obtained by hydro- or solvothermal treatment of nitrogen-containing molecules, like amino acids or EDTA. *N*-CDs can be obtained also by multicomponent synthesis, in which a precursor without nitrogen atoms (e.g., citric acid) is allowed to react in the presence of a doping agent (e.g., ethylenediamine or urea) to afford *N*-CDs.[178] In these systems, which were studied in great detail if compared to others, heteroatom doping results in improved PL characteristics that were associated with the formation of molecular-like fluorophores in *a*-CDs, while the emission was attributed to *N*-centered defects of graphitic domains in *g*-CDs.[170,179] Further studies evidenced how molecular fluorophores are produced in the reaction of citric acid and ethylenediamine at 200°C. Amidation and cyclization reactions led to the formation of 5-oxo-1,2,3,5-tetrahydroimidazo[1,2-α]pyridine-7-carboxylic acid (IPCA), which is a highly fluorescent molecule and was detected in the analysis of the reaction products by the means of different

techniques. IPCA was identified as the responsible of the luminescent properties of the material, albeit it is still unclear if it is covalently bonded to the polymeric chains of these *N*-CDs or absorbed in their structure. This study also enlightened the need for reliable purification protocols to eliminate low molecular weight impurities, as well as larger particles deriving from the synthesis of *N*-CDs.[180] The use of a doping agent is usually associated with an increase of the PL features, a trend also linked to the amount of nitrogen introduced in the system. As an example, it was observed that the quantum yield of *N*-CDs, obtained from citric acid in the presence of different doping agents, increases dramatically. In this study, three different doping agents were assessed: ammonium hydroxide, ethylenediamine, and diethylenetriamine. The non-doped CDs were characterized by a quantum yield lower than 1%, while *N*-CDs were characterized by an increased quantum yield of 15.6% and 56.8% by using ethylenediamine and diethylenetriamine, respectively.[181] We recently reported a synthetic protocol of *N*-CDs using arginine and ethylenediamine (Figure 16a). Also in this case the use of a doping agent resulted in excellent PL characteristics of the so-obtained material, which was characterized by a diameter size of 2.5 ± 0.8 nm as determined *via* atomic force microscopy (AFM). The overall quantum yield was 17% and, after separation by the means of size exclusion chromatography it was obtained a fraction of *N*-CDs with higher luminescence (quantum yield of 46%). The presence of primary amino groups on the surface of *N*-CDs was detected with the Kaiser test. This analysis evidenced the presence of 1350 µmol/g amino groups. Moreover, these surface functionalities conferred to the as obtained *N*-CDs excellent solubility in water and mild solubility in organic solvents like DMF and DMSO. However, as indicated by XPS analysis, different types of nitrogen are also present in the structure. Despite obtaining more detailed structural information still represents a challenge, we were able to establish the different contributions of arginine and ethylenediamine in the resulting material. Comparative NMR experiments performed on materials obtained with ^{13}C labelled precursors evidenced how arginine contributes mainly to the signals associated with aromatic domains, while ethylenediamine was found to be responsible for the signals attributed to aliphatic groups.[33,182] The concept of using a doping agent to fine-tune the properties of the resulting CDs has proven to be a highly convenient and flexible route. By the means of this approach, *N*-CDs with unique and outstanding features can be obtained, like in the work in which ethylenediamine was replaced with a chiral doping agent. In the synthesis of *N*-CDs with (*S*)-arginine and ethylenediamine, the chirality of the amino acid is lost due to high temperature (above 200°C) that results in racemization. The replacement of ethylenediamine with (*R,R*)- and (*S,S*)-cyclohexanediamine resulted in the retention of chirality in the obtained *N*-CDs (Figure 16b). Both electronic and vibration dichroism analyses were conducted, and the chiral nature of this kind of *N*-CDs, albeit with low intensity signals, was detected. The introduction of chirality in this nanomaterial opens up exciting perspectives for their exploitation in fields where chirality is a crucial aspect, like medicinal chemistry.[183]

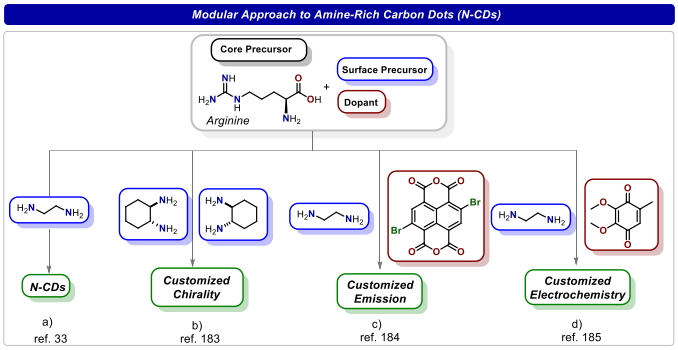

Figure 16: a) Schematic representation of the synthesis of *N*-CDs from arginine and ethylenediamine, b) one-pot doping with a chiral diamine c) one-pot doping with NDI, d) one-pot doping with quinones

Several other examples of one-pot functionalization were reported and, in this context, the versatile reactivity of the amino group played a major role in these syntheses. White light-emitting *N*-CDs were obtained by reaction of arginine, ethylenediamine, and naphthalene dianhydrides (NDI) in an MW-assisted protocol. The reaction of the amino groups with the anhydride moieties, affording the corresponding imides, allowed us to fine-tune the emission color of the material ranging from blue to orange. When bromine core-substituted NDI were used, aromatic nucleophilic substitution between amino groups and the bay positions of NDI contributed to the *N*-CDs formation and by tuning the equivalents of precursors we were able to obtain white light-emitting *N*-CDs (Figure 16c).[184] The one-pot functionalization of *N*-CDs can be exploited not only for the tailoring of the chiral and optical properties of these materials.

We have also shown how the introduction of quinones in the arginine/ethylenediamine based *N*-CDs synthesis can influence the redox characteristics of the resulting material (Figure 16d). The formation of imines between amines and quinones and their consequent inclusion in the *N*-CDs structure resulted in the modulation of their redox potential, from -1.52 to -2.04 V vs SCE (standard calomelane electrode).[185] Other methods for the tuning of *N*-CDs features rely on a more traditional post-synthetic functionalization by exploiting the classic reactivity of the amino group, whose presence allows to covalently attach ligands on the surface of the material.[186] This method is particularly convenient when the one-pot functionalization could not be exploited due to degradation or interference of the dopant in the formation process of *N*-CDs. Many examples of post-synthetic functionalization are described in literature and exploit the well-known chemistry of the amino group, like the reaction between amines and thiocyanates,[187] sulfonyl chloride derivatives[188] and with activated carboxylates by exploiting ethyl(dimethylaminopropyl)carbodiimide (EDC) / *N*-hydroxysuccinimide (NHS) coupling agents.[189,190] This versatile toolbox for post-synthetic functionalization has been widely used for the derivatization of *N*-CDs allowing the synthesis of nanohybrids with unique properties. As an example, this method was used for the synthesis of nanohybrids between *N*-CDs and porphyrins. In this work, we covalently linked a carboxylic acid tetraphenyl porphyrin derivative *via* amidic

coupling (Figure 17). The resulting material was characterized by a good aqueous solubility and, interestingly, it was observed to undergo charge separated states upon light excitation, opening new perspectives for the application of this material in energy conversion technologies.[191] The introduction of amino groups in CDs has proven to be an effective strategy for tailoring their properties, and the methods described in this section, namely heteroatom doping, one-pot functionalization, and post-synthetic functionalization, significantly widened the range of opportunities to modulate the characteristics of this class of nanomaterial, opening new and exciting opportunities for the development of new technologies based on *N*-CDs.

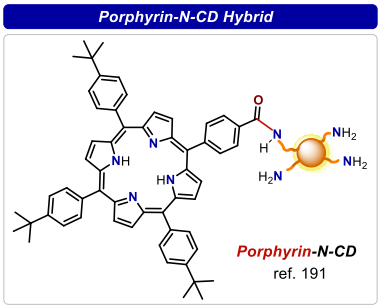

Figure 17: the *N*-CDs/porphyrin nanohybrid obtained *via* amidic coupling.

2.5.2. Applications of *N*-CDs

CDs, since their serendipitous discovery, have emerged as a very promising scaffold for many applications, with an always growing number of reports in which CDs are successfully employed. One of the most important properties of *N*-CDs is their biocompatibility. Several studies have demonstrated how this material has an intrinsic low cytotoxicity[192] and for this reason is extensively studied for biomedical applications like biosensing[193] and bioimaging.[194] Indeed, the presence of amino groups on the surface of *N*-CDs offers the opportunity to use this material for advanced applications. For instance, we exploited the amino groups of *N*-CDs to covalently bond a chemotherapeutic agent, paclitaxel, characterized by high toxicity and very poor aqueous solubility. This molecule was allowed to react at the hydroxyl group present at the C2' position with succinic anhydride and the free carboxyl group was further reacted with *N*-CDs *via* amide bond exploiting EDC and NHS coupling agents (Figure 18). The hybrid was then tested in cellular assays that evidenced an increased apoptotic activity compared to the drug alone in breast (MCF-7 and MDA-MB-231), lung (A-549), prostate (PC-3) and cervix (HeLa and C33-A) cancer cell lines. Because it is known that derivatization of paclitaxel at the 2' hydroxyl position results in a loss of activity, the observed apoptotic activity is probably expressed after ester hydrolysis that allows the release of the drug. This nanohybrid can be regarded in this context as a prodrug. The PL properties of the *N*-CDs/paclitaxel adduct allowed also to detect cell internalization as well as their localization inside the cells. This example shows how *N*-CDs can be successfully used as a scaffold for theranostic applications and for the delivery of poorly soluble anticancer drugs.[195]

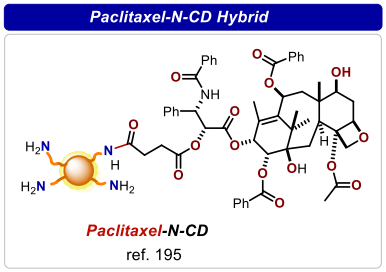

Figure 18: The paclitaxel/*N*-CDs nanohybrid for drug delivery applications.

N-CDs can also be incorporated into a hybrid diimidazolium based ionogel. The resulting ionogels showed the characteristic emission of *N*-CDs and displayed an improved antioxidant activity compared to the single components. Moreover, their ability to self-repairing was observed.[196]

The reactivity of amino groups present on the surface of *N*-CDs can be exploited not only to covalently graft molecular species but in principle, can also be utilized to achieve chemical transformations. The possibility of exploitation of this nanomaterial in photo- or organocatalysis was therefore explored. So far, however, only a few examples of CDs promoted catalysis are reported,[197,198] among which an example of how *N*-CDs can be used for the photocatalytic perfluoroalkylation of electron-rich substrates (Figure 19). In this case, the perfluoroalkylation of the substrates was achieved thanks to the combination of two events: 1) the halogen bond interaction between the *σ*-hole of iodoperfluoroalkyl chains and the lone pair of amino groups on the surface of *N*-CDs, detected by the means of ^{19}F-NMR technique, and 2) the generation of a highly reactive perfluoroalkyl radical (**V**) caused by the electron transfer with the excited state of *N*-CDs. Many electron-rich substrates were perfluoroalkylated with this method including phenols, olefins, and caffeine. Overall, this strategy allowed the formation of C-C bonds under mild and operationally simple conditions.[17]

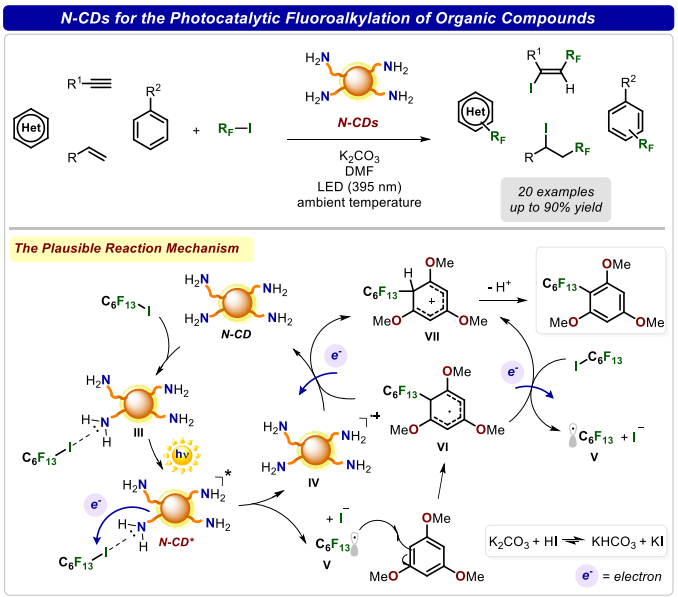

Figure 19: *N*-CDs mediated photocatalytic perfluoroalkylation.

Moretto *et al.* have shown how the same *N*-CDs can be incorporated into four different polymeric matrixes, namely polyester-amide, polyurea-urethane, polyamide, and polymethyl methacrylate (PMMA) by interfacial polymerization. The resulting hybrid materials retained the properties of pristine *N*-CDs and were used for the photoreduction of silver ions to silver nanoparticles and the photo-oxidation of benzyl alcohol to benzaldehyde under visible light at 405 nm in presence of H_2O_2.[199]

CDs are being extensively studied for photovoltaic applications,[200] and the production of processable *N*-CDs/PMMA composites was also exploited.[201] Solution blending PMMA with a *N*-CDs loading of 0.1 and 0.01 wt.% conferred the characteristic PL features of *N*-CDs to the composite, with a strong emission band at 400 and 450 nm upon light excitation at 300 and 320 nm, respectively. These novel nanocomposites were found to be very promising candidates for the performance improvement of silicon-based solar cells by converting UV light to visible light.[201]

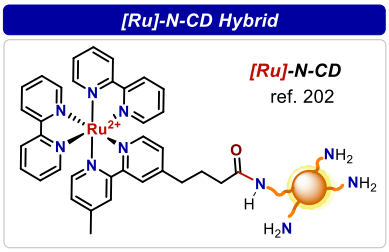

Figure 20: The ruthenium(II)tris(2,2'-bipyridyl)-*N*-CDs nanohybrid for ECL generation.

N-CDs express a wide potential in energy-related applications. For instance, a ruthenium(II)tris(2,2'-bipyridyl) ($Ru(bpy)_3^{2+}$) complex has been covalently grafted to *N*-CDs through carboxylic acid-amine coupling (Figure 20). The resulting nanohybrid was characterized by excellent electrochemiluminescent properties (ECL). For the achievement of ECL, oxidizable co-reactants, like the corrosive and volatile tripropylamine, are usually required in high concentrations. But in this case, the proximity of the two components allowed an intramolecular electron transfer. As a result, the use of co-reactants was avoided.[202]

3. Outlook and perspectives

In this Feature Article, we describe our approach toward the introduction of amino groups onto CNMs. From the discussion above, it is quite clear that the synthesis and production of amino-functionalized carbon nanostructures is an extremely useful approach for practical applications, which span from nanomedicine to materials science to catalysis, etc. The covalent functionalization of nanostructures with amino groups can be implemented using a wide variety of organic reactions, affording new materials with tuneable properties. There is no doubt that other elements, like sulfur-containing molecules, can be inserted onto CNMs.[112,203,204] However, the amino group is still dominating the field of covalent functionalization, due to its high versatility and to its peculiar features, providing new fascinating characteristics to the carbon nanostructures. Nowadays, the functionalization is carried out with standard protocols, namely 1,3-dipolar cycloaddition of azomethine ylides or the radical arylation reaction, but the discovery of new synthetic pathways carried out in milder and eco-friendly conditions for large scale production is desirable. Nonetheless, it would be fundamental to find new chemical and spectroscopic techniques for precise and reliable quantification of amino moieties, discriminating them from impurities. This last point is of extreme importance, due to the continuous emergence of more and more smart nanohybrids and bioconjugated nanostructures. This is particularly true for the synthesis of nanohybrids with CDs, where the amino groups are not only powerful tools for the production of new nanostructures, but also the starting building blocks that tailor the functionalities for an *ad hoc* material. In the current nanotechnological era, CNMs represent a landmark for the growth of this research field. Certainly, they will still play a determinant role also in the coming future. As time goes by, new exciting nanoshapes continue to be discovered and new nanomaterials with surprising chemical characteristics are yet to come.[205] However, the real utilization of these nanomaterials needs to pass through the customization: the doping and functionalization, in particular with amine-based compounds, are pushing forward this process, making available their final commercialization.

Conflicts of interest

There are no conflicts to declare.

Acknowledgements

M. P. is the AXA Chair for Carbon Bionanotechnology (2016-2023). This work was supported by the University of Trieste, INSTM, the Italian Ministry of Education MIUR (cofin Prot. 2017PBXPN4), and the Spanish Ministry of Science, Innovation and Universities, MICIU (project PID2019-108523RB-I00). Part of this work was performed under the Maria de Maeztu Units of Excellence Program from the Spanish State Research Agency Grant no. MDM-2017-0720.

Notes and references

1 *Nat. Nanotechnol.*, 2016, **11**, 828–834.
2 M. C. Roco, *AIChE J.*, 2004, **50**, 890–897.
3 V. Georgakilas, J. A. Perman, J. Tucek and R. Zboril, *Chem. Rev.*, 2015, **115**, 4744–4822.
4 H. W. Kroto, J. R. Heath, S. C. O'Brien, R. F. Curl and R. E. Smalley, *Nature*, 1985, **318**, 162–163.
5 S. Iijima, *Nature*, 1991, **354**, 56–58.
6 S. Iijima and T. Ichihashi, *Nature*, 1993, **363**, 603–605.
7 K. S. Novoselov, A. K. Geim, S. V. Morozov, D. Jiang, Y. Zhang, S. V. Dubonos, I. V. Grigorieva and A. A. Firsov, *Science*, 2004, **306**, 666–669.
8 X. Xu, R. Ray, Y. Gu, H. J. Ploehn, L. Gearheart, K. Raker and W. A. Scrivens, *J. Am. Chem. Soc.*, 2004, **126**, 12736–12737.

9 E. Vázquez, F. Giacalone and M. Prato, *Chem. Soc. Rev.*, 2014, **43**, 58–69.

10 H. Ali-Boucetta, A. Nunes, R. Sainz, M. A. Herrero, B. Tian, M. Prato, A. Bianco and K. Kostarelos, *Angew. Chem. Int. Ed.*, 2013, **52**, 2274–2278.

11 R. C. Haddon, *Science*, 1993, **261**, 1545–1550.

12 Z. Chen, W. Thiel and A. Hirsch, *ChemPhysChem*, 2003, **4**, 93–97.

13 M. Quintana, E. Vazquez and M. Prato, *Acc. Chem. Res.*, 2013, **46**, 138–148.

14 M. Maggini, G. Scorrano and M. Prato, *J. Am. Chem. Soc.*, 1993, **115**, 9798–9799.

15 L. Maggini, J. Ahrens-Jensen, G. Lo Re, J. M. Raquez, P. Dubois and D. Bonifazi, *Carbon*, 2014, **70**, 22–29.

16 M. I. Lucío, F. Pichler, J. R. Ramírez, A. de la Hoz, A. Sánchez-Migallón, C. Hadad, M. Quintana, A. Giulani, M. V. Bracamonte, J. L. G. Fierro, C. Tavagnacco, M. A. Herrero, M. Prato and E. Vázquez, *Chem. – A Eur. J.*, 2016, **22**, 8879–8888.

17 C. Rosso, G. Filippini and M. Prato, *Chem. – A Eur. J.*, 2019, **25**, 16032–16036.

18 D. Pantarotto, R. Singh, D. McCarthy, M. Erhardt, J.-P. Briand, M. Prato, K. Kostarelos and A. Bianco, *Angew. Chem. Int. Ed.*, 2004, **43**, 5242–5246.

19 D. Pantarotto, C. D. Partidos, R. Graff, J. Hoebeke, J.-P. Briand, M. Prato and A. Bianco, *J. Am. Chem. Soc.*, 2003, **125**, 6160–6164.

20 C. Ménard-Moyon, C. Fabbro, M. Prato and A. Bianco, *Chem. – A Eur. J.*, 2011, **17**, 3222–3227.

21 C. Hadad, X. Ke, M. Carraro, A. Sartorel, C. Bittencourt, G. Van Tendeloo, M. Bonchio, M. Quintana and M. Prato, *Chem. Commun.*, 2014, **50**, 885–887.

22 F. Kunc, V. Balhara, A. Brinkmann, Y. Sun, D. M. Leek and L. J. Johnston, *Anal. Chem.*, 2018, **90**, 13322–13330.

23 M. S. Dresselhaus, A. Jorio and R. Saito, *Annu. Rev. Condens. Matter Phys.*, 2010, **1**, 89–108.

24 D. Parviz, F. Irin, S. A. Shah, S. Das, C. B. Sweeney and M. J. Green, *Adv. Mater.*, 2016, **28**, 8796–8818.

25 D. R. Baer, M. H. Engelhard, G. E. Johnson, J. Laskin, J. Lai, K. Mueller, P. Munusamy, S. Thevuthasan, H. Wang, N. Washton, A. Elder, B. L. Baisch, A. Karakoti, S. V. N. T. Kuchibhatla and D. Moon, *J. Vac. Sci. Technol. A*, 2013, **31**, 050820.

26 G. Bottari, M. Á. Herranz, L. Wibmer, M. Volland, L. Rodríguez-Pérez, D. M. Guldi, A. Hirsch, N. Martín, F. D'Souza and T. Torres, *Chem. Soc. Rev.*, 2017, **46**, 4464–4500.

27 S. Kralj, M. Drofenik and D. Makovec, *J. Nanoparticle Res.*, 2011, **13**, 2829–2841.

28 Y. Sun, F. Kunc, V. Balhara, B. Coleman, O. Kodra, M. Raza, M. Chen, A. Brinkmann, G. P. Lopinski and L. J. Johnston, *Nanoscale Adv.*, 2019, **1**, 1598–1607.

29 R. Suzuki and H. Konno, *ACS Appl. Mater. Interfaces*, 2020, **22**, 3309–3312.

30 E. Kaiser, R. L. Colescott, C. D. Bossinger and P. I. Cook, *Anal. Biochem.*, 1970, **34**, 595–598.

31 J. D. Fontenot, J. M. Ball, M. A. Miller, C. M. David and R. C. Montelaro, *Pept. Res.*, 1991, **4**, 19–25.

32 M. Quintana, K. Spyrou, M. Grzelczak, W. R. Browne, P. Rudolf and M. Prato, *ACS Nano*, 2010, **4**, 3527–3533.

33 F. Arcudi, L. Đorđević and M. Prato, *Angew. Chem. Int. Ed.*, 2016, **55**, 2107–2112.

34 P. R. Buseck, S. J. Tsipursky and R. Hettich, *Science*, 1992, **257**, 215–217.

35 J. Cami, J. Bernard-Salas, E. Peeters and S. E. Malek, *Science*, 2010, **329**, 1180–1182.

36 F. Diederich, R. Ettl, Y. Rubin, R. L. Whetten, R. Beck, M. Alvarez, S. Anz, D. Sensharma, F. Wudl, K. C. Khemani and A. Koch, *Science*, 1991, **252**, 548–551.

37 D. M. Guldi and M. Prato, *Acc. Chem. Res.*, 2000, **33**, 695–703.

38 M. Prato and M. Maggini, *Acc. Chem. Res.*, 1998, **31**, 519–526.

39 T. Hashimoto and K. Maruoka, *Chem. Rev.*, 2015, **115**, 5366–5412.

40 N. Tagmatarchis and M. Prato, *Synlett*, 2003, 768–779.

41 K. Kordatos, S. Bosi, T. Da Ros, A. Zambon, V. Lucchini and M. Prato, *J. Org. Chem.*, 2001, **66**, 2802–2808.

42 S. Marchesan, T. Da Ros and M. Prato, *J. Org. Chem.*, 2005, **70**, 4706–4713.

43 C. Thilgen, A. Herrmann and F. Diederich, *Angew. Chem. Int. Ed.*, 1997, **36**, 2268–2280.

44 N. Martín, M. Altable, S. Filippone, A. Martín-Domenech, L. Echegoyen and C. M. Cardona, *Angew. Chem. Int. Ed.*, 2006, **45**, 110–114.

45 I. Guryanov, A. Montellano López, M. Carraro, T. Da Ros, G. Scorrano, M. Maggini, M. Prato and M. Bonchio, *Chem. Commun.*, 2009, 3940–3942.

46 A. Bianco, M. Maggini, G. Scorrano, C. Toniolo, G. Marconi, C. Villani and M. Prato, *J. Am. Chem. Soc.*, 1996, **118**, 4072–4080.

47 F. Novello, M. Prato, T. Da Ros, M. De Amici, A. Bianco, C. Toniolo and M. Maggini, *Chem. Commun.*, 1996, 903–904.

48 S. Filippone, E. E. Maroto, Á. Martín-Domenech, M. Suarez and N. Martín, *Nat. Chem.*, 2009, **1**, 578–582.

49 E. E. Maroto, A. de Cózar, S. Filippone, Á. Martín-Domenech, M. Suarez, F. P. Cossío and N. Martín, *Angew. Chem. Int. Ed.*, 2011, **50**, 6060–6064.

50 K. Sawai, Y. Takano, M. Izquierdo, S. Filippone, N. Martín, Z. Slanina, N. Mizorogi, M. Waelchli, T. Tsuchiya, T. Akasaka and S. Nagase, *J. Am. Chem. Soc.*, 2011, **133**, 17746–17752.

51 E. E. Maroto, S. Filippone, A. Martín-Domenech, M. Suarez and N. Martín, *J. Am. Chem. Soc.*, 2012, **134**, 12936–12938.

52 J. Marco-Martínez, V. Marcos, S. Reboredo, S. Filippone and N. Martín, *Angew. Chem. Int. Ed.*, 2013, **52**, 5115–5119.

53 J. Marco-Martínez, S. Reboredo, M. Izquierdo, V. Marcos, J. L. López, S. Filippone and N. Martín, *J. Am. Chem. Soc.*, 2014, **136**, 2897–2904.

54 J. M. Fernández-García, P. J. Evans, S. Filippone, M. Á. Herranz and N. Martín, *Acc. Chem. Res.*, 2019, **52**, 1565–1574.

55 K.-F. Liou and C.-H. Cheng, *Chem. Commun.*, 1996, 1423–1424.

56 X. Zhang, M. Willems and C. S. Foote, *Tetrahedron Lett.*, 1993, **34**, 8187–8188.

57 M. Iyoda, F. Sultana and M. Komatsu, *Chem. Lett.*, 1995, **24**,

1133–1134.
58 M. Maggini and E. Menna, in *Fullerenes: From Synthesis to Optoelectronic Properties.*, Springer, Dordrecht, 2002, pp. 1–50.
59 C. F. Richardson, D. I. Schuster and S. R. Wilson, *Org. Lett.*, 2000, **2**, 1011–1014.
60 I. Guryanov, F. M. Toma, A. Montellano López, M. Carraro, T. Da Ros, G. Angelini, E. D'Aurizio, A. Fontana, M. Maggini, M. Prato and M. Bonchio, *Chem. – A Eur. J.*, 2009, **15**, 12837–12845.
61 A. Bagno, S. Claeson, M. Maggini, M. L. Martini, M. Prato and G. Scorrano, *Chem. – A Eur. J.*, 2002, **8**, 1015–1023.
62 T. Da Ros, M. Prato, M. Carano, P. Ceroni, F. Paolucci and S. Roffia, *J. Am. Chem. Soc.*, 1998, **120**, 11645–11648.
63 M. Carano, T. Da Ros, M. Fanti, K. Kordatos, M. Marcaccio, F. Paolucci, M. Prato, S. Roffia and F. Zerbetto, *J. Am. Chem. Soc.*, 2003, **125**, 7139–7144.
64 M. Carano, P. Ceroni, F. Paolucci, S. Roffia, T. Da Ros, M. Prato, M. I. Sluch, C. Pearson, M. C. Petty and M. R. Bryce, *J. Mater. Chem.*, 2000, **10**, 269–273.
65 A. Mateo-Alonso, C. Sooambar and M. Prato, *Org. Biomol. Chem.*, 2006, **4**, 1629–1637.
66 F. Pellarini, D. Pantarotto, T. Da Ros, A. Giangaspero, A. Tossi and M. Prato, *Org. Lett.*, 2001, **3**, 1845–1847.
67 D. Pantarotto, A. Bianco, F. Pellarini, A. Tossi, A. Giangaspero, I. Zelezetsky, J.-P. Briand and M. Prato, *J. Am. Chem. Soc.*, 2002, **124**, 12543–12549.
68 S. Bosi, L. Feruglio, T. Da Ros, G. Spalluto, B. Gregoretti, M. Terdoslavich, G. Decorti, S. Passamonti, S. Moro and M. Prato, *J. Med. Chem.*, 2004, **47**, 6711–6715.
69 S. H. Friedman, D. L. DeCamp, R. P. Sijbesma, G. Srdanov, F. Wudl and G. L. Kenyon, *J. Am. Chem. Soc.*, 1993, **115**, 6506–6509.
70 S. Marchesan, T. Da Ros, G. Spalluto, J. Balzarini and M. Prato, *Bioorg. Med. Chem. Lett.*, 2005, **15**, 3615–3618.
71 G. Pastorin, S. Marchesan, J. Hoebeke, T. Da Ros, L. Ehret-Sabatier, J. P. Briand, M. Prato and A. Bianco, *Org. Biomol. Chem.*, 2006, **4**, 2556–2562.
72 E. Nakamura, H. Isobe, N. Tomita, M. Sawamura, S. Jinno and H. Okayama, *Angew. Chem. Int. Ed.*, 2000, **39**, 4254–4257.
73 C. Klumpp, L. Lacerda, O. Chaloin, T. Da Ros, K. Kostarelos, M. Prato and A. Bianco, *Chem. Commun.*, 2007, 3762–3764.
74 V. Campisciano, M. Gruttadauria and F. Giacalone, *ChemCatChem*, 2019, **11**, 90–133.
75 J. López-Andarias, A. Frontera and S. Matile, *J. Am. Chem. Soc.*, 2017, **139**, 13296–13299.
76 C. Rosso, M. G. Emma, A. Martinelli, M. Lombardo, A. Quintavalla, C. Trombini, Z. Syrgiannis and M. Prato, *Adv. Synth. Catal.*, 2019, **361**, 2936–2944.
77 D. Jariwala, V. K. Sangwan, L. J. Lauhon, T. J. Marks and M. C. Hersam, *Chem. Soc. Rev.*, 2013, **42**, 2824–2860.
78 C. H. Lee, G. Yu, D. Moses, V. I. Srdanov, X. Wei and Z. V. Vardeny, *Phys. Rev. B*, 1993, **48**, 8506–8509.
79 S. Collavini and J. L. Delgado, *Sustain. Energy Fuels*, 2018, **2**, 2480–2493.
80 C. M. Atienza, G. Fernández, L. Sánchez, N. Martín, I. S. Dantas, M. M. Wienk, R. A. J. Janssen, G. M. A. Rahman and D. M. Guldi, *Chem. Commun.*, 2006, 514–516.
81 V. Sgobba, G. Giancane, S. Conoci, S. Casilli, G. Ricciardi, D. M. Guldi, M. Prato and L. Valli, *J. Am. Chem. Soc.*, 2007, **129**, 3148–3156.
82 S. Bettini, S. Sawalha, L. Carbone, G. Giancane, M. Prato and L. Valli, *Nanoscale*, 2019, **11**, 7414–7423.
83 N. Martín and J. F. Nierengarten, *Supramolecular Chemistry of Fullerenes and Carbon Nanotubes*, Wiley-VCH Verlag GmbH & Co. KGaA, Weinheim, Germany, 2012.
84 L. Đorđević, T. Marangoni, F. De Leo, I. Papagiannouli, P. Aloukos, S. Couris, E. Pavoni, F. Monti, N. Armaroli, M. Prato and D. Bonifazi, *Phys. Chem. Chem. Phys.*, 2016, **18**, 11858–11868.
85 M. Barrejón, A. Mateo-Alonso and M. Prato, *Eur. J. Org. Chem.*, 2019, 2019, 3371–3383.
86 A. Mateo-Alonso, C. Ehli, G. M. A. Rahman, D. M. Guldi, G. Fioravanti, M. Marcaccio, F. Paolucci and M. Prato, *Angew. Chem. Int. Ed.*, 2007, **46**, 3521–3525.
87 M. Carini, T. Da Ros, M. Prato and A. Mateo-Alonso, *ChemPhysChem*, 2016, **17**, 1823–1828.
88 D. S. Bethune, C. H. Kiang, M. S. de Vries, G. Gorman, R. Savoy, J. Vazquez and R. Beyers, *Nature*, 1993, **363**, 605–607.
89 R. Saito, M. Fujita, G. Dresselhaus and M. S. Dresselhaus, *Appl. Phys. Lett.*, 1992, **60**, 2204–2206.
90 L. Dai, D. W. Chang, J.-B. Baek and W. Lu, *Small*, 2012, **8**, 1130–1166.
91 M. F. L. De Volder, S. H. Tawfick, R. H. Baughman and A. J. Hart, *Science*, 2013, **339**, 535–539.
92 V. Schroeder, S. Savagatrup, M. He, S. Lin and T. M. Swager, *Chem. Rev.*, 2019, **119**, 599–663.
93 D. M. Guldi and N. Martín, *Carbon Nanotubes and Related Structures*, Wiley-VCH Verlag GmbH & Co. KGaA, 2010.
94 D. Tasis, N. Tagmatarchis, A. Bianco and M. Prato, *Chem. Rev.*, 2006, **106**, 1105–1136.
95 J. L. Bahr, J. Yang, D. V Kosynkin, M. J. Bronikowski, R. E. Smalley and J. M. Tour, *J. Am. Chem. Soc.*, 2001, **123**, 6536–6542.
96 M. S. Strano, C. A. Dyke, M. L. Usrey, P. W. Barone, M. J. Allen, H. Shan, C. Kittrell, R. H. Hauge, J. M. Tour and R. E. Smalley, *Science*, 2003, **301**, 1519–1522.
97 J. L. Bahr and J. M. Tour, *Chem. Mater.*, 2001, **13**, 3823–3824.
98 M. E. Lipińska, S. L. H. Rebelo, M. F. R. Pereira, J. A. N. F. Gomes, C. Freire and J. L. Figueiredo, *Carbon*, 2012, **50**, 3280–3294.
99 V. Georgakilas, K. Kordatos, M. Prato, D. M. Guldi, M. Holzinger and A. Hirsch, *J. Am. Chem. Soc.*, 2002, **124**, 760–761.
100 V. Georgakilas, N. Tagmatarchis, D. Pantarotto, A. Bianco, J.-P. Briand and M. Prato, *Chem. Commun.*, 2002, 3050–3051.
101 P. Singh, S. Campidelli, S. Giordani, D. Bonifazi, A. Bianco and M. Prato, *Chem. Soc. Rev.*, 2009, **38**, 2214–2230.
102 C. A. Dyke and J. M. Tour, *J. Am. Chem. Soc.*, 2003, **125**, 1156–1157.
103 F. G. Brunetti, M. A. Herrero, J. de M. Muñoz, S. Giordani, A. Díaz-Ortiz, S. Filippone, G. Ruaro, M. Meneghetti, M. Prato and E. Vázquez, *J. Am. Chem. Soc.*, 2007, **129**, 14580–14581.

104 K. M. Lee, L. Li and L. Dai, *J. Am. Chem. Soc.*, 2005, **127**, 4122–4123.

105 G. Pastorin, W. Wu, S. Wieckowski, J.-P. Briand, K. Kostarelos, M. Prato and A. Bianco, *Chem. Commun.*, 2006, 1182–1184.

106 J. J. Stephenson, J. L. Hudson, A. D. Leonard, B. K. Price and J. M. Tour, *Chem. Mater.*, 2007, **19**, 3491–3498.

107 F. G. Brunetti, M. A. Herrero, J. de M. Muñoz, A. Díaz-Ortiz, J. Alfonsi, M. Meneghetti, M. Prato and E. Vázquez, *J. Am. Chem. Soc.*, 2008, **130**, 8094–8100.

108 B. K. Price and J. M. Tour, *J. Am. Chem. Soc.*, 2006, **128**, 12899–12904.

109 B. K. Price, J. L. Hudson and J. M. Tour, *J. Am. Chem. Soc.*, 2005, **127**, 14867–14870.

110 M. Barrejón, Z. Syrgiannis and M. Prato, *Nanoscale*, 2018, **10**, 15782–15787.

111 Z. Syrgiannis, V. La Parola, C. Hadad, M. Lucío, E. Vázquez, F. Giacalone and M. Prato, *Angew. Chem. Int. Ed.*, 2013, **52**, 6480–6483.

112 Z. Syrgiannis, A. Bonasera, E. Tenori, V. La Parola, C. Hadad, M. Gruttadauria, F. Giacalone and M. Prato, *Nanoscale*, 2015, **7**, 6007–6013.

113 C. Gaillard, G. Cellot, S. Li, F. M. Toma, H. Dumortier, G. Spalluto, B. Cacciari, M. Prato, L. Ballerini and A. Bianco, *Adv. Mater.*, 2009, **21**, 2903–2908.

114 R. Singh, D. Pantarotto, D. McCarthy, O. Chaloin, J. Hoebeke, C. D. Partidos, J.-P. Briand, M. Prato, A. Bianco and K. Kostarelos, *J. Am. Chem. Soc.*, 2005, **127**, 4388–4396.

115 A. Bianco, J. Hoebeke, S. Godefroy, O. Chaloin, D. Pantarotto, J.-P. Briand, S. Muller, M. Prato and C. D. Partidos, *J. Am. Chem. Soc.*, 2005, **127**, 58–59.

116 M. A. Herrero, F. M. Toma, K. T. Al-Jamal, K. Kostarelos, A. Bianco, T. Da Ros, F. Bano, L. Casalis, G. Scoles and M. Prato, *J. Am. Chem. Soc.*, 2009, **131**, 9843–9848.

117 J. E. Podesta, K. T. Al-Jamal, M. A. Herrero, B. Tian, H. Ali-Boucetta, V. Hegde, A. Bianco, M. Prato and K. Kostarelos, *Small*, 2009, **5**, 1176–1185.

118 M. Prato, K. Kostarelos and A. Bianco, *Acc. Chem. Res.*, 2008, **41**, 60–68.

119 D. Iannazzo, A. Pistone, S. Galvagno, S. Ferro, L. De Luca, A. M. Monforte, T. Da Ros, C. Hadad, M. Prato and C. Pannecouque, *Carbon*, 2015, **82**, 548–561.

120 W. Wu, S. Wieckowski, G. Pastorin, M. Benincasa, C. Klumpp, J.-P. Briand, R. Gennaro, M. Prato and A. Bianco, *Angew. Chem. Int. Ed.*, 2005, **44**, 6358–6362.

121 V. Lovat, D. Pantarotto, L. Lagostena, B. Cacciari, M. Grandolfo, M. Righi, G. Spalluto, M. Prato and L. Ballerini, *Nano Lett.*, 2005, **5**, 1107–1110.

122 V. Martinelli, G. Cellot, F. M. Toma, C. S. Long, J. H. Caldwell, L. Zentilin, M. Giacca, A. Turco, M. Prato, L. Ballerini and L. Mestroni, *Nano Lett.*, 2012, **12**, 1831–1838.

123 S. Bosi, A. Fabbro, C. Cantarutti, M. Mihajlovic, L. Ballerini and M. Prato, *Carbon*, 2016, **97**, 87–91.

124 S. Bosi, R. Rauti, J. Laishram, A. Turco, D. Lonardoni, T. Nieus, M. Prato, D. Scaini and L. Ballerini, *Sci. Rep.*, 2015, **5**, 9562.

125 V. Martinelli, S. Bosi, B. Peña, G. Baj, C. S. Long, O. Sbaizero, M. Giacca, M. Prato and L. Mestroni, *ACS Appl. Bio Mater.*, 2018, **1**, 1530–1537.

126 B. Peña, S. Bosi, B. A. Aguado, D. Borin, N. L. Farnsworth, E. Dobrinskikh, T. J. Rowland, V. Martinelli, M. Jeong, M. R. G. Taylor, C. S. Long, R. Shandas, O. Sbaizero, M. Prato, K. S. Anseth, D. Park and L. Mestroni, *ACS Appl. Mater. Interfaces*, 2017, **9**, 31645–31656.

127 A. Servant, I. Jacobs, C. Bussy, C. Fabbro, T. da Ros, E. Pach, B. Ballesteros, M. Prato, K. Nicolay and K. Kostarelos, *Carbon*, 2016, **97**, 126–133.

128 M. Melchionna, S. Marchesan, M. Prato and P. Fornasiero, *Catal. Sci. Technol.*, 2015, **5**, 3859–3875.

129 F. M. Toma, A. Sartorel, M. Iurlo, M. Carraro, P. Parisse, C. MacCato, S. Rapino, B. R. Gonzalez, H. Amenitsch, T. Da Ros, L. Casalis, A. Goldoni, M. Marcaccio, G. Scorrano, G. Scoles, F. Paolucci, M. Prato and M. Bonchio, *Nat. Chem.*, 2010, **2**, 826–831.

130 A. Sartorel, M. Carraro, G. Scorrano, R. De Zorzi, S. Geremia, N. D. McDaniel, S. Bernhard and M. Bonchio, *J. Am. Chem. Soc.*, 2008, **130**, 5006–5007.

131 F. Giacalone, V. Campisciano, C. Calabrese, V. La Parola, Z. Syrgiannis, M. Prato and M. Gruttadauria, *ACS Nano*, 2016, **10**, 4627–4636.

132 L. Chen, Y. Hernandez, X. Feng and K. Müllen, *Angew. Chem. Int. Ed.*, 2012, **51**, 7640–7654.

133 P. Wick, A. E. Louw-Gaume, M. Kucki, H. F. Krug, K. Kostarelos, B. Fadeel, K. A. Dawson, A. Salvati, E. Vázquez, L. Ballerini, M. Tretiach, F. Benfenati, E. Flahaut, L. Gauthier, M. Prato and A. Bianco, *Angew. Chem. Int. Ed.*, 2014, **53**, 7714–7718.

134 D. S. Su, S. Perathoner and G. Centi, *Chem. Rev.*, 2013, **113**, 5782–5816.

135 S. Wu, Q. He, C. Tan, Y. Wang and H. Zhang, *Small*, 2013, **9**, 1160–1172.

136 F. Bonaccorso, Z. Sun, T. Hasan and A. C. Ferrari, *Nat. Photonics*, 2010, **4**, 611–622.

137 M. Pumera, *Energy Environ. Sci.*, 2011, **4**, 668–674.

138 M. Cai, D. Thorpe, D. H. Adamson and H. C. Schniepp, *J. Mater. Chem.*, 2012, **22**, 24992–25002.

139 J. M. Tour, *Chem. Mater.*, 2014, **26**, 163–171.

140 V. L. Nguyen and Y. H. Lee, *Small*, 2015, **11**, 3512–3528.

141 V. León, M. Quintana, M. A. Herrero, J. L. G. Fierro, A. de la Hoz, M. Prato and E. Vázquez, *Chem. Commun.*, 2011, **47**, 10936–10938.

142 A. Ciesielski and P. Samorì, *Chem. Soc. Rev.*, 2014, **43**, 381–398.

143 A. Criado, M. Melchionna, S. Marchesan and M. Prato, *Angew. Chem. Int. Ed.*, 2015, **54**, 10734–10750.

144 J. Kim, S. Kwon, D.-H. Cho, B. Kang, H. Kwon, Y. Kim, S. O. Park, G. Y. Jung, E. Shin, W.-G. Kim, H. Lee, G. H. Ryu, M. Choi, T. H. Kim, J. Oh, S. Park, S. K. Kwak, S. W. Yoon, D. Byun, Z. Lee and C. Lee, *Nat. Commun.*, 2015, **6**, 8294.

145 V. León, J. M. González-Domínguez, J. L. G. Fierro, M. Prato and E. Vázquez, *Nanoscale*, 2016, **8**, 14548–14555.

146 T. Kuila, S. Bose, A. K. Mishra, P. Khanra, N. H. Kim and J. H. Lee, *Prog. Mater. Sci.*, 2012, **57**, 1061–1105.

147 D. W. Johnson, B. P. Dobson and K. S. Coleman, *Curr. Opin. Colloid Interface Sci.*, 2015, **20**, 367–382.

148 Y. Hernandez, V. Nicolosi, M. Lotya, F. M. Blighe, Z. Sun, S. De, I. T. McGovern, B. Holland, M. Byrne, Y. K. Gun'Ko, J. J.

Boland, P. Niraj, G. Duesberg, S. Krishnamurthy, R. Goodhue, J. Hutchison, V. Scardaci, A. C. Ferrari and J. N. Coleman, *Nat. Nanotechnol.*, 2008, **3**, 563–568.
149 M. Quintana, A. Montellano, A. E. del Rio Castillo, G. Van Tendeloo, C. Bittencourt and M. Prato, *Chem. Commun.*, 2011, **47**, 9330–9332.
150 R. Sharma, J. H. Baik, C. J. Perera and M. S. Strano, *Nano Lett.*, 2010, **10**, 398–405.
151 M. Z. Hossain, M. A. Walsh and M. C. Hersam, *J. Am. Chem. Soc.*, 2010, **132**, 15399–15403.
152 X. Ke, S. Turner, M. Quintana, C. Hadad, A. Montellano-López, M. Carraro, A. Sartorel, M. Bonchio, M. Prato, C. Bittencourt and G. Van Tendeloo, *Small*, 2013, **9**, 3922–3927.
153 M. S. Dresselhaus and G. Dresselhaus, *Adv. Phys.*, 1981, **30**, 139–326.
154 C. Vallés, C. Drummond, H. Saadaoui, C. A. Furtado, M. He, O. Roubeau, L. Ortolani, M. Monthioux and A. Pénicaud, *J. Am. Chem. Soc.*, 2008, **130**, 15802–15804.
155 J. M. Englert, C. Dotzer, G. Yang, M. Schmid, C. Papp, J. M. Gottfried, H.-P. Steinrück, E. Spiecker, F. Hauke and A. Hirsch, *Nat. Chem.*, 2011, **3**, 279–286.
156 H.-L. Hou, J. P. Merino, A. Criado, A. Hirsch and M. Prato, *2D Mater.*, 2019, **6**, 25009.
157 Y. Cheng, Y. Fan, Y. Pei and M. Qiao, *Catal. Sci. Technol.*, 2015, **5**, 3903–3916.
158 M. Quintana, A. M. López, S. Rapino, F. M. Toma, M. Iurlo, M. Carraro, A. Sartorel, C. Maccato, X. Ke, C. Bittencourt, T. Da Ros, G. Van Tendeloo, M. Marcaccio, F. Paolucci, M. Prato and M. Bonchio, *ACS Nano*, 2013, **7**, 811–817.
159 X. Ke, S. Turner, M. Quintana, C. Hadad, A. Montellano-López, M. Carraro, A. Sartorel, M. Bonchio, M. Prato, C. Bittencourt and G. Van Tendeloo, *Small*, 2013, **9**, 3922–3927.
160 J. P. Merino, S. Serna, A. Criado, A. Centeno, I. Napal, J. Calvo, A. Zurutuza, N. Reichardt and M. Prato, *2D Mater.*, 2020, **7**, 24003.
161 H. Li, Z. Kang, Y. Liu and S. T. Lee, *J. Mater. Chem.*, 2012, **22**, 24230–24253.
162 Y. Park, J. Yoo, B. Lim, W. Kwon and S.-W. Rhee, *J. Mater. Chem. A*, 2016, **4**, 11582–11603.
163 F. Arcudi, L. Đorđević and M. Prato, *Acc. Chem. Res.*, 2019, **52**, 2070–2079.
164 P. Zhu, K. Tan, Q. Chen, J. Xiong and L. Gao, *Chem. Mater.*, 2019, **31**, 4732–4742.
165 N. Papaioannou, A. Marinovic, N. Yoshizawa, A. E. Goode, M. Fay, A. Khlobystov, M.-M. Titirici and A. Sapelkin, *Sci. Rep.*, 2018, **8**, 6559.
166 S. N. Baker and G. A. Baker, *Angew. Chem. Int. Ed.*, 2010, **49**, 6726–6744.
167 S. Yatom, J. Bak, A. Khrabryi and Y. Raitses, *Carbon*, 2017, **117**, 154–162.
168 S.-L. Hu, K.-Y. Niu, J. Sun, J. Yang, N.-Q. Zhao and X.-W. Du, *J. Mater. Chem.*, 2009, **19**, 484–488.
169 H. Li, R. Liu, W. Kong, J. Liu, Y. Liu, L. Zhou, X. Zhang, S.-T. Lee and Z. Kang, *Nanoscale*, 2014, **6**, 867–873.
170 A. Sciortino, A. Cannizzo and F. Messina, *C*, 2018, **4**, 67.
171 P. Yang, J. Zhao, L. Zhang, L. Li and Z. Zhu, *Chem. - A Eur. J.*, 2015, **21**, 8561–8568.
172 Y. Xu, M. Wu, Y. Liu, X.-Z. Feng, X.-B. Yin, X.-W. He and Y.-K. Zhang, *Chem. - A Eur. J.*, 2013, **19**, 2276–2283.
173 Q.-Q. Shi, Y.-H. Li, Y. Xu, Y. Wang, X.-B. Yin, X.-W. He and Y.-K. Zhang, *RSC Adv.*, 2014, **4**, 1563–1566.
174 X. Meng, Y. Wang, X. Liu, M. Wang, Y. Zhan, Y. Liu, W. Zhu, W. Zhang, L. Shi and X. Fang, *Opt. Mater. (Amst).*, 2018, **77**, 48–54.
175 S. Sahu, B. Behera, T. K. Maiti and S. Mohapatra, *Chem. Commun.*, 2012, **48**, 8835–8837.
176 G. A. M. Hutton, B. C. M. Martindale and E. Reisner, *Chem. Soc. Rev.*, 2017, **46**, 6111–6123.
177 L. Li and T. Dong, *J. Mater. Chem. C*, 2018, **6**, 7944–7970.
178 D. Li, P. Jing, L. Sun, Y. An, X. Shan, X. Lu, D. Zhou, D. Han, D. Shen, Y. Zhai, S. Qu, R. Zbořil and A. L. Rogach, *Adv. Mater.*, 2018, **30**, 1705913.
179 V. Strauss, J. T. Margraf, C. Dolle, B. Butz, T. J. Nacken, J. Walter, W. Bauer, W. Peukert, E. Spiecker, T. Clark and D. M. Guldi, *J. Am. Chem. Soc.*, 2014, **136**, 17308–17316.
180 J. Schneider, C. J. Reckmeier, Y. Xiong, M. Von Seckendorff, A. S. Susha, P. Kasak and A. L. Rogach, *J. Phys. Chem. C*, 2017, **121**, 2014–2022.
181 J. Manioudakis, F. Victoria, C. A. Thompson, L. Brown, M. Movsum, R. Lucifero and R. Naccache, *J. Mater. Chem. C*, 2019, **7**, 853–862.
182 L. Đorđević, F. Arcudi and M. Prato, *Nat. Protoc.*, 2019, **14**, 2931–2953.
183 L. Đorđević, F. Arcudi, A. D'Urso, M. Cacioppo, N. Micali, T. Bürgi, R. Purrello and M. Prato, *Nat. Commun.*, 2018, **9**, 3442.
184 F. Arcudi, L. Đorđević and M. Prato, *Angew. Chem. Int. Ed.*, 2017, **56**, 4170–4173.
185 F. Rigodanza, L. Đorđević, F. Arcudi and M. Prato, *Angew. Chem. Int. Ed.*, 2018, **57**, 5062–5067.
186 W. Liu, C. Li, Y. Ren, X. Sun, W. Pan, Y. Li, J. Wang and W. Wang, *J. Mater. Chem. B*, 2016, **4**, 5772–5788.
187 F. Du, Y. Ming, F. Zeng, C. Yu and S. Wu, *Nanotechnology*, 2013, **24**, 365101.
188 Z. Ye, R. Tang, H. Wu, B. Wang, M. Tan and J. Yuan, *New J. Chem.*, 2014, **38**, 5721–5726.
189 Y. Yan, J. Sun, K. Zhang, H. Zhu, H. Yu, M. Sun, D. Huang and S. Wang, *Anal. Chem.*, 2015, **87**, 2087–2093.
190 X. Cui, L. Zhu, J. Wu, Y. Hou, P. Wang, Z. Wang and M. Yang, *Biosens. Bioelectron.*, 2015, **63**, 506–512.
191 F. Arcudi, V. Strauss, L. Đorđević, A. Cadranel, D. M. Guldi and M. Prato, *Angew. Chem. Int. Ed.*, 2017, **56**, 12097–12101.
192 J. Wang and J. Qiu, *J. Mater. Sci.*, 2016, **51**, 4728–4738.
193 J. Zhang and S.-H. Yu, *Mater. Today*, 2016, **19**, 382–393.
194 Y. Song, S. Zhu and B. Yang, *RSC Adv.*, 2014, **4**, 27184–27200.
195 I. J. Gomez, B. Arnaiz, M. Cacioppo, F. Arcudi and M. Prato, *J. Mater. Chem. B*, 2018, **6**, 5540–5548.
196 C. Rizzo, F. Arcudi, L. Đorđević, N. T. Dintcheva, R. Noto, F. D'Anna and M. Prato, *ACS Nano*, 2018, **12**, 1296–1305.
197 C. Testa, A. Zammataro, A. Pappalardo and G. Trusso Sfrazzetto, *RSC Adv.*, 2019, **9**, 27659–27664.
198 C. Rosso, G. Filippini and M. Prato, *ACS Catal.*, 2020, 8090–8105.

199 D. Mosconi, D. Mazzier, S. Silvestrini, A. Privitera, C. Marega, L. Franco and A. Moretto, *ACS Nano*, 2015, **9**, 4156–4164.
200 J. B. Essner and G. A. Baker, *Environ. Sci. Nano*, 2017, **4**, 1216–1263.
201 F. Amato, M. Cacioppo, F. Arcudi, M. Prato, M. Mituo, E. G. Fernandes, M. N. P. Carreño, I. Pereyra and J. R. Bartoli, *Chem. Eng. Trans.*, 2019, **74**, 1105–1110.
202 S. Carrara, F. Arcudi, M. Prato and L. De Cola, *Angew. Chem. Int. Ed.*, 2017, **56**, 4757–4761.
203 H. Omachi, T. Inoue, S. Hatao, H. Shinohara, A. Criado, H. Yoshikawa, Z. Syrgiannis and M. Prato, *Angew. Chem. Int. Ed.*, 2020, **59**, 7836–7841.
204 J. M. González-Domínguez, A. Santidrián, A. Criado, C. Hadad, M. Kalbáč and T. Da Ros, *Chem. - A Eur. J.*, 2015, **21**, 18631–18641.
205 W. Gibbs, *Science*, DOI:10.1126/science.aba1927.